urticaria and pruritus, to more severe reactions, such as cardiopulmonary arrest and even death [11]. However, because mild ARs are generally tolerated, and moderate-to-severe reactions are very rare, as many as 60 million doses of iodinated CM are used worldwide each year [12].

Although the etiology of many or most hypersensitivity reactions is unknown, an allergic-like mechanism appears to be engaged in some patients because allergic individuals or patients with asthma are considered to be at an increased risk for developing AR [13]. Therefore, it is possible that repeated exposures to iodinated CM increase the risk of AR by a mechanism based on sensitization. Especially, HCC patients, who receive multiple injections to CM, are likely to be put at the risk of ARs. However, to our knowledge, no reports have investigated whether the risk of ARs increases with the cumulative number of examinations with iodinated CM in individual patients with HCC.

The aim of this study was to evaluate the risk factors for AR to non-ionic iodinated CM, among a large number of contrast-enhanced computed tomography (CT) examinations and, and to elucidate whether repeated exposures to CM increase the risk of AR upon subsequent exposure in patients with HCC.

Materials and Methods

Ethic statement

This retrospective study was conducted according to the ethical guidelines for epidemiological research designed by the Japanese Ministry of Education, Culture, Sports, Science and Technology and Ministry of Health, Labour, and Welfare. The study design was included in a comprehensive protocol of retrospective study at the Department of Gastroenterology, The University of Tokyo Hospital approved by The University of Tokyo Medical Research Center Ethics Committee (approval number 2058). The following statements were posted at a website (http://gastro.m.u-tokyo.ac.jp/med/0602A.htm) and participants who do not agree to the use of their clinical data can claim deletion of them.

Department of Gastroenterology at The University of Tokyo Hospital contains data from our daily practice for the assessment of short-term (treatment success, immediate adverse events etc.) and long-term (late complications, recurrence etc.) outcomes. Obtained data were stored in an encrypted hard disk separated from outside of the hospital. When reporting analyzed data, we protect the anonymity of participants for the sake of privacy protection. If you do not wish the utilization of your data for the clinical study or have any question on the research content, please do not hesitate to make contact with us.

Patients

The medical records of 1,861 consecutive patients with HCC who visited the authors' institution between January 1, 2004 and December 31, 2008 were reviewed retrospectively. Most of these patients received contrast-enhanced CT examinations on a regular basis for the assessment of disease status, including HCC recurrence. We counted the number of cumulative contrast-enhanced CT examinations and transarterial chemoembolization (TACE) treatments with intra-arterial infusion of iodinated CM, until death, drop-out, or December 31, 2011, whichever came first.

We collected the following data recorded on the application form for contrast-enhanced CT or TACE: sex, age, past history of ARs to iodinated CM, past history of asthma, history of other allergies, corticosteroid use and the presence of renal impairment, defined as an estimated glomerular filtration rate (eGFR) < 60 ml min−1, as an indicator of chronic renal insufficiency [14]. We also evaluated hepatic function based on the Child-Pugh classification (CPC) [15] to assess its association with the incidence of AR.

Contraindications for contrast media administrations and prophylaxis

Pregnant women, patients with previous severe AR to CM and patient with severe thyroid disease are contraindicated to administration of CM at our institution. Patients with asthma, renal impairment, severe heart disease, macroglobulinemia, multiple myeloma and pheochromocytoma are also in principle excluded from an indication for CM administration. However, in clinical practice, patients with these impairments or diseases sometimes receive CM when the clinical advantages outweigh the potential toxicity.

Corticosteroid is sometimes given prophylactically to patients with previous mild AR to CM and patients with mild asthma when they are exposed to iodinated CM. In this study, the decision whether or not to utilize corticosteroid prophylaxis was made by individual clinicians, based on the available information [16–18].

Contrast-enhanced CT and TACE

All contrast-enhanced CT examinations and TACE, performed on HCC patients at the authors' hospital from January 1, 2004 through December 31, 2011, were identified by means of an electronic query to the institutional database system. The following non-ionic low osmolality CM had been in use: iopamidol 300-mg iodine per mL (Iopamiron 300; Nihon Schering, Osaka, Japan), iopamidol 370-mg iodine per mL (Iopamiron 370; Nihon Schering, Osaka, Japan), or iohexol 350-mg iodine per mL (Omnipaque 350; Daiichi Sankyo, Tokyo, Japan). The choice of iodinated CM depended on the protocol and the attending physician. When a patient with a previous immediate AR to iopamidol required further examination, we switched to iohexol and vice versa in accordance with the guidelines set forth by the European Society of Urogenital Radiology [19].

CT scanning was performed according to standard clinical protocols. The standard volume of 2 mL kg−1, to a maximum of 100 mL, was injected at a rate of 2.3–3.3 mL s−1 with a power injector. All patients were monitored closely during injection. If any symptom was observed during or immediately after CM injection, the clinician or radiologist checked the patient's vital signs and performed a physical examination.

TACE was performed under local anesthesia. A catheter was inserted into the hepatic artery via the femoral artery. When hypervascular tumors were identified during the hepatic angiography procedure, the feeding arteries were selectively

embolized with gelatin sponge particles after an emulsion of epirubicin hydrochloride (Pharmorubicin; Pfizer Japan, Tokyo, Japan), and iodized oil (Lipiodol Ultra-Fluid; Schering Japan, Osaka, Japan) was injected under X-ray monitoring.

Contrast-enhanced MRI and contrast-enhanced ultrasonography at our institution

Contrast-enhanced magnetic resonance imaging (MRI) and contrast-enhanced ultrasonography (CEUS) are efficient tools for detecting HCC [20,21]. However, MRI requires more time than CT, and there are fewer MRI devices than CTs in our institution. Thus, we were compelled to limit the number of patients examined by MRI. Along with B-mode ultrasonography, a comprehensive assessment of the whole liver by CEUS may sometimes be hampered by the patient's body habitus, colonic interposition, or morphologic changes by cirrhosis, which leads to decreasing the ability of detecting small HCCs [22]. Accordingly, contrast-enhanced CT is the first choice for diagnosis of HCC and follow-up after the therapy at our institution unless the patient has contraindication for iodinated CM administration. We sequentially use contrast-enhanced MRI or CEUS for the difficult cases to distinguish HCC from benign nodules [23] or to detect HCC by only dynamic CT [24].

Adverse reactions to contrast media

This study was focused on ARs related to iodinated CM. However, it is difficult to discriminate between ARs to CM and accidental events. Therefore, after considerable preliminary evaluation of the data, we concluded that the following view of ARs was useful and statistically sound. First, we evaluated any symptom as an AR, regardless of whether the symptom was attributable to CM, to the procedure, or an accidental event. Second, we categorized all symptoms into hypersensitivity reactions, physiologic reactions, and 'other' reactions, according to the American College of Radiology (ACR) guidelines, and evaluated each category as an event [25]. Hypersensitivity reactions included skin symptoms such as pruritus and urticaria, angioedema (such as a scratchy throat, slight throat and/or facial swelling), bronchospasm, and anaphylactoid shock, that is, hypotension with tachycardia. ACR guidelines categorized paroxysmal sneezing as a hypersensitivity reaction. However, due to the difficulty in distinguishing between allergic sneezing and coincidence, we categorized all sneezing into other reactions. Other reactions, not specifically outlined in the ACR guidelines, but that were sometimes observed in this study, were defined as symptoms that were observed immediately after CM injection, although it was unclear whether the symptoms were related to CM injections. Specifically, this category included sneezing and cough. The severity of ARs to iodinated CM was classified according to ACR guidelines.

The radiologists and physicians attending the CT examination and TACE reported on the manifestation and severity of the AR, and whether the patient received medical treatment. These data were fed immediately into the electronic medical record system shared by hospital staff. If more than one manifestation of the AR to a single CM injection was identified, we chose the most severe reaction as the manifestation.

Subsequent contrast media injections and adverse reactions to them

Some patients who exhibited an AR subsequently received another CM injection and experienced subsequent ARs. Thus, we investigated the association between the initial ARs and the reactions to subsequent injections. We also elucidated manifestations and the severity of subsequent reactions and, if present, incremented its severity.

Statistical method

We retrospectively collected the demographic and laboratory data that were available 2 weeks before the initial CM examination. The difference was assessed using the Mann–Whitney U-test for continuous data; the chi-squared test or Fisher's exact test was used for categorical data. The cumulative probability curves were constructed using the method of Kaplan–Meier, which were compared with the log-rank test. We also analyzed the cumulative incidence of ARs with respect to each AR category described above (i.e., allergic, physiologic, or other) and compared this using the log-rank test. We did not treat these categories as competing risks, because these reactions may have occurred at a single administration.

To investigate whether the risk of AR increased with accumulated exposure to CM, we analyzed the relationship between the hazard function for AR to CM and the number of cumulative exposures to CM. The hazard function, defined as $h(t) = -S'(t)/S(t)$, where $S(t)$ is the survival function, and $S'(t)$ its derivative, is a measure of the tendency for the event to occur. By calculating the hazard function for the occurrence of AR, with respect to the number of previous exposures as a function of time, we can evaluate whether or not the number of previous exposures affected the immediate risk of AR. In this analysis, the cumulative number of exposures to CM had a major influence on the results. Thus, we calculated the hazard functions for only the 'exposure-naïve' patients, defined as those who had their initial injection of iodinated CM during the study period. Additionally, we used restricted quadratic splines in the Poisson-rate regression model, with three knots at the 10th, 50th, and 90th percentiles of the number of cumulative exposures to CM, to investigate the possible nonlinear relationship between the number of cumulative exposures to CM and the hazard function [26,27].

Risk factors for AR were analyzed by univariate and multivariate Cox proportional hazard-regression models. A stepwise variable selection was performed with Akaike Information Criteria in a multivariate analysis. The results of the multivariate analyses were presented as hazard ratios (HR), with their corresponding 95% confidence intervals (CI) and P values from the Wald test.

In clinical practice, we often do not know the cumulative number of iodinated CM injections a patient has been administered; but instead, are aware of the presence or absence of past injection. Hence, we included past exposure to iodinated CM before the study period as a covariate, in addition

Table 1. Baseline characteristics.

Characteristic		n = 1,729
Age (y)	Median (IQR)	69 (62-74)
	Range	22-93
Male sex, n (%)		1,156 (66.9)
Absence of previous iodinated contrast media injections, n (%)		973 (56.3)
History of adverse reaction to iodinated contrast media, n (%)		45 (2.6)
History of allergy, n (%)		164 (9.5)
History of asthma, n (%)		23 (1.3)
Use of corticosteroid at entry, n (%)		28 (1.6)
Child–Pugh classification, n (%)		
A		1427 (82.5)
B or C		302 (17.5)
Renal function at entry		
eGFR (ml/min), Median (IQR)		73.6 (61.7-87.3)
Presence of renal impairment, n (%)		383 (22.2)

doi: 10.1371/journal.pone.0076018.t001

to the following variables: age (as a continuous number), sex, presence of a previous AR to iodinated CM, presence of allergy, presence of asthma, presence of renal impairment, defined as an estimated glomerular filtration rate (eGFR) < 60 ml min−1, as an indicator of chronic renal insufficiency [28], presence of corticosteroid use, and CPC A vs. B or C.

Statistical analyses were performed using R 2.13.0 (http://www.R-project.org) and SAS (Cary, NC). All tests were two-sided, with $P < 0.05$ denoting statistical significance.

Results

Overall, 1,861 patients with HCC were reviewed, of which 132 were excluded because they were given no CM during the study period. The baseline characteristics of the remaining 1,729 (92.9%) patients are summarized in Table 1. Nine hundred and seventy-three (56.3%) patients had no exposure to iodinated CM. Forty-five (2.6%) of 1,729 patients had a previous history of ARs to CM and 164 (9.5%) had a history of allergy.

Manifestations and severity of adverse reactions

A total of 23,684 iodinated CM examinations were performed in the 1,729 patients during the study period; the total number of ARs were recorded for 196 (0.83% on an injection basis and 11.3% on a patient basis) examinations.

The manifestations and severity of the recorded ARs are summarized in Table 2. Sixty-two patients developed hypersensitivity reactions. The most common manifestation of a hypersensitivity reaction was urticaria, which occurred locally in 25 patients and systemically in nine. There were two severe ARs: both were anaphylactoid shock. Seventy-one patients developed physiologic reactions. The most common symptoms were digestive manifestations, such as nausea or vomiting, which occurred in 35 patients. There were 58 other reactions and we could not know the manifestation of AR in 7 patients. Two patients developed both hypersensitivity and physiologic reactions (one had pruritus and dizziness, and another had nausea and pruritus). The number of CT examinations and TACE and the observed ARs are also provided separately in Table 2. Significantly more ARs were observed in TACE than during CT (0.78% vs. 1.60%, $P = 0.0017$). This difference was attributed to the number of physiologic reactions, in particular, vasovagal reflux (0.22% vs. 1.53%, $P < 0.001$).

Additionally, we analyzed the cumulative probability of AR by drawing a cumulative probability curve over the number of cumulative exposures. The cumulative probabilities of overall immediate reaction at the 10th, 20th, and 30th contrast-enhanced CT examinations were 7.9%, 15.2%, and 24.1%, respectively (Figure 1A). Cumulative probabilities of a hypersensitivity reaction at the 10th, 20th, and 30th contrast-enhanced CT examinations were 2.5%, 5.4%, and 7.8%, respectively, whereas the cumulative probabilities of a physiologic reaction at the 10th, 20th, and 30th injections were 3.4%, 5.2%, and 8.4%, respectively. Cumulative probabilities of other reactions at the 10th, 20th, and 30th injections were 2.1%, 4.9%, and 9.0%, respectively (Figure 1B).

Longitudinal changes in hazard of adverse reaction

We analyzed the hazard of ARs to CM in 973 exposure-naïve patients. The estimated hazard of overall AR gradually decreased until around the 10th exposure, and then increased thereafter (Figure 2A). The hazard function of hypersensitivity reaction demonstrated a V-shaped change with cumulative number of exposures (Figure 2B). The hazard function of physiologic reactions plateaued or decreased with increasing number of exposures to CM (Figure 2C). Risk of other reactions increased with cumulative number of exposures (Figure 2D).

Table 2. Manifestations and severities of overall adverse reactions (ARs) and ARs during contrast-enhanced computed tomography and transarterial chemoembolization.

		Overall		Enhanced CT		TACE		*P* value
		n = 23,684		n = 22,185		n = 1,499		
Patients with any immediate symptom, n (%)		196	(0.83)	172	(0.78)	24	(1.60)	0.0017
Hypersensitivity reaction, n (%)		62	(0.26)	61	(0.28)	1	(0.07)	0.19
Mild	Local urticaria, n (%)	25	(0.11)	25	(0.11)	0	(0.00)	0.40
	Pruritus, n(%)	8	(0.03)	8	(0.04)	0	(0.00)	1.00
	Scratchy throat, n (%)	7	(0.03)	7	(0.03)	0	(0.00)	1.00
Moderate	Systemic urticaria, n (%)	9	(0.04)	9	(0.04)	0	(0.00)	1.00
	Hypotension with tachycardia, n (%)	3	(0.01)	3	(0.01)	0	(0.00)	1.00
	Dyspnea/Bronchospasm, n (%)	8	(0.03)	8	(0.04)	0	(0.00)	1.00
Severe	Anaphylactoid shock with loss of consciousness, n (%)	1	(0.00)*	1	(0.00)*	0	(0.00)	1.00
	Anaphylactoid shock with convulsion, n (%)	1	(0.00)*	0	(0.00)	1	(0.07)	0.063
Physiologic reaction, n (%)		71	(0.30)	48	(0.22)	23	(1.53)	<0.001
Mild	Nausea/Vomiting, n (%)	35	(0.15)	29	(0.12)	6	(0.40)	0.021
	Dizziness, n (%)	5	(0.02)	5	(0.02)	0	(0.00)	1.00
	Flush, n (%)	4	(0.02)	4	(0.01)	0	(0.00)	1.00
	Sensation of warmth, n (%)	5	(0.02)	5	(0.01)	0	(0.00)	1.00
	Headache, n (%)	1	(0.00)*	1	(0.00)*	0	(0.00)	1.00
	Chest pain, n (%)	1	(0.00)*	1	(0.00)*	0	(0.00)	1.00
Moderate	Hypotension, n (%)	5	(0.02)	0	(0.00)	5	(0.33)	<0.001
	Hypertension, n (%)	1	(0.00)*	0	(0.00)	1	(0.07)	0.063
	Vasovagal reflux, n (%)	12	(0.05)	1	(0.00)*	11	(0.73)	<0.001
	Tachycardia, n (%)	1	(0.00)*	1	(0.00)*	0	(0.00)	1.00
	Severe vomiting, n (%)	1	(0.00)*	1	(0.00)*	0	(0.00)	1.00
Other, n (%)		58	(0.24)	58	(0.26)	0	(0.00)	0.051
	Sneezing, n (%)	39	(0.16)	39	(0.18)	0	(0.00)	0.18
	Cough, n (%)	19	(0.08)	19	(0.09)	0	(0.00)	0.63
Unknown, n (%)		7	(0.03)	7	(0.03)	0	(0.00)	1.00

Abbreviations: CT, computed tomography; TACE, transarterial chemoembolization.

*. Less than 0.005%.

Note: Two patients had both hypersensitivity and physiologic reactions to a single exposure.

The difference in the adverse reaction rate was assessed by Fisher's exact test.

doi: 10.1371/journal.pone.0076018.t002

Risk factors for adverse reactions

In multivariate analysis with stepwise variable selection, the presence of previous iodinated CM exposure (HR: 1.41; 95% CI: 1.05, 1.90; P = 0.022), presence of renal impairment (HR: 1.65; 95% CI: 1.17, 2.32; P = 0.0040), previous AR to iodinated CM (HR: 2.60; 95% CI: 1.32, 5.13; P = 0.0056), past history of asthma (HR: 2.81; 95% CI: 1.32, 5.99; P = 0.0076), and past history of allergies other than iodinated contrast media (HR: 1.87; 95% CI: 1.32, 2.67; P <0.001) were found to be significant risk factors (Figure 3).

Subsequent contrast media injections and adverse reactions to them

Subsequent injections after the initial AR and ARs to subsequent injections are summarized in Figure 4. During the study period, initial ARs to iodinated CM occurred in 196 patients, 61 (31.1%) of whom did not receive further injections of iodinated CM. When patients with AR to iodinated CM were repeatedly re-injected, subsequent ARs occurred at high rates (36.9%). Re-injections of iodinated CM and ARs to them showed some trends. First, when the initial reaction was hypersensitivity, the patients were less likely to receive subsequent injections of iodinated CM (hypersensitivity vs. physiologic + other, 48.4% vs. 77.5%, respectively). When they did, corticosteroid was likely used as the prophylaxis when iodinated CM were re-injected (hypersensitivity vs. physiologic + other, 53.3% vs. 9.0%, respectively). Second, most recurrent ARs were classified into the same category as the initial reaction. The concordance rate for classification of the initial and subsequent reaction was 79.1%. Finally, only one case showed a subsequent AR that was more severe than the initial reaction. In this case, the patient had local urticaria as the initial reaction and systemic urticaria as the subsequent reaction. In contrast, two patients had subsequent reactions milder than the initial one. One patient had hypotension with tachycardia as the initial reaction and dizziness as the second. The other patient had systemic urticaria as the initial reaction and facial urticaria as the subsequent reaction with corticosteroid.

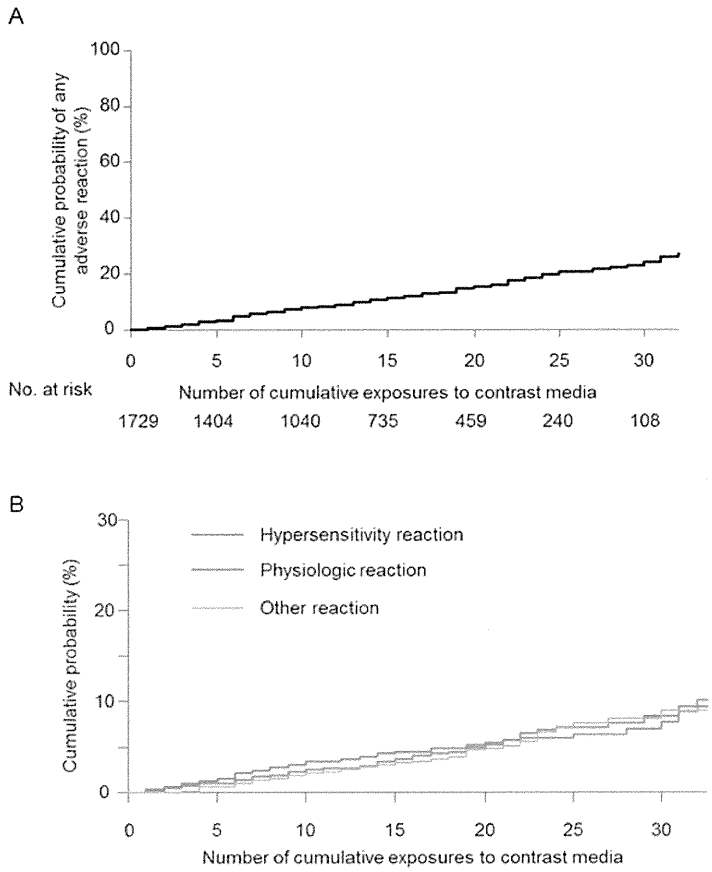

Figure 1. The cumulative probabilities of overall and each reactions to iodinated contrast media. Graphs illustrate (A) the cumulative probability of overall adverse reactions to iodinated contrast media and (B) the cumulative probabilities of hypersensitivity, physiologic and other adverse reactions to iodinated contrast media.

doi: 10.1371/journal.pone.0076018.g001

Discussion

Although there are many reports of CM for CT, the current study is, to our knowledge, the first to report the cumulative effect of repeated iodinated CM injections on immediate ARs.

According to the hazard functions of AR analyzed in this study, the risk of ARs seemed to change biphasically (Figure 2A); the decreasing phase occurred during the first 10 injections, followed by an increasing phase. The decreasing phase may indicate that a portion of the patients were intrinsically sensitive to iodinated CM and had ARs at an earlier examination. In contrast, the increasing phase may reflect the cumulative effects of repeated CM injections.

By separate analyses for each AR category, we showed that the increasing phase consisted of hypersensitivity reaction and other reaction. Therefore, the risk of hypersensitivity reaction to iodinated contrast media accumulates with increasing number of exposures to CM. From the viewpoint of the cumulative effects of repeated exposures to CM, other reactions had similar properties to the hypersensitivity reactions. In this study, sneezing was classified as an 'other' reaction. However, given that paroxysmal sneezing is classified as a hypersensitivity reaction according to the ACR guidelines, a portion of the sneezing reactions may be caused by an allergic-like mechanism. Therefore, it was plausible that other reactions had similar properties to the hypersensitivity reactions.

In accordance with previous reports (8,18), the history of previous AR to CM, and the presence of asthma and other allergic diseases, were risk factors for ARs to CM. Patients with prior severe AR to CM or severe asthma were ineligible for CM injections and may have been excluded from this study cohort, resulting in a selection bias. Nevertheless, these variables were identified as risk factors for ARs to CM by use of a multivariate Cox proportional hazard regression model. This reinforced the strong associations between the ARs and these factors.

This present study also showed that the cumulative probability of ARs were significantly higher in patients with renal impairment than in patients with normal renal function (Figure 3). We could not explain the definite reason. However,

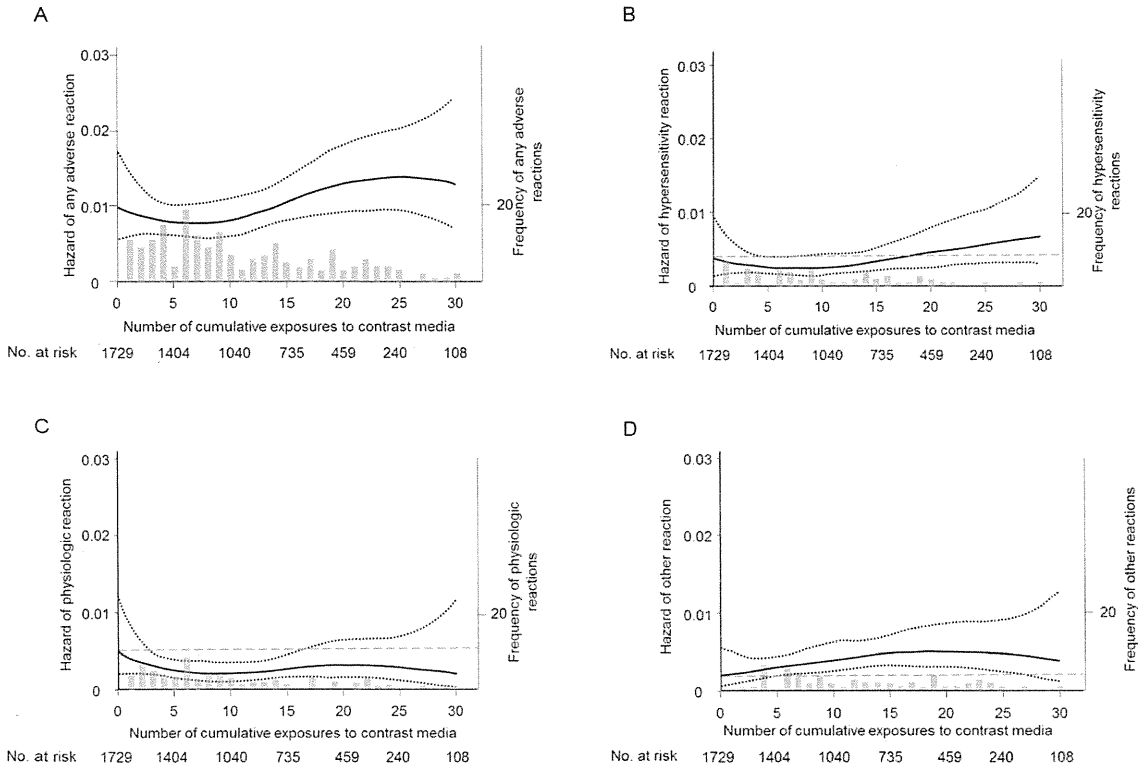

Figure 2. The smoothed plots of the estimated hazard of overall and each reactions to iodinated contrast media. The curves illustrate smoothed plot of the estimated hazard of (A) overall adverse reactions, (B) hypersensitivity, (C) physiologic and (D) other adverse reaction to iodinated contrast media in patients with no previous exposure to contrast media. The hazard function (solid line) and 95% confidence intervals (black dotted line) were estimated by a smoothing spline with three knots. Gray dotted lines show the hazard at the initial exposure.

doi: 10.1371/journal.pone.0076018.g002

we speculated that serum osmolality may increase at a relatively higher rate in patients with renal impairment than if a decrease in the eGFR level was due to hypovolemia, leading to strengthening osmotoxicity. Patients with renal impairment were expected to have fewer CM injections than patients with normal renal function because the renal function of such patients further deteriorated over a natural course, and these patients were contraindicated for CM injection. Thus, the incidence probability of ARs in patients with renal impairment may have been underestimated. Nonetheless, patients with renal impairment had significantly more frequent ARs than patients with normal renal function.

When patients with AR to iodinated CM were repeatedly re-injected with CM, subsequent ARs occurred at high rates (36.7%) (Figure 4). Previous reports showed that repeat CM reaction in premedicated patients, i.e., breakthrough reactions, were usually similar in severity to the initial reaction [29,30]. The results of this study are compatible with these previous reports.

This study has some limitations. First, the data set was obtained from a single institution and reviewed retrospectively, leading to an underestimation of the true incidence of ARs, due to the tendencies of retrospective investigations. Second, we admit that several patients may have received intravenous CM at other institutions, and developed an AR without our knowledge. Third, we did not evaluate other risk factors, such as the use of beta-adrenergic blockers [31,32]. Fourth, patients with the high risk factors such as severe asthma or other allergic diseases were possibly excluded from this study cohort. Fifth, this study has a low statistical power for very rare ARs like anaphylactoid shock. Sixth, we estimated the cumulative incidence and hazard of adverse reactions on the assumption that the risk of subsequent ARs is similar between TACE and contrast-enhanced CT, which is in fact controversial. The SCVIR study conducted by Bettmann et al. showed equal incidence of ARs after intra-arterial and intravenous administration of CM [33]. In contrast, others reported that intra-arterial administration of CM was accompanied by lower risk of ARs [34,35]. However, these reports estimated the risk of ARs to a single exposure only and did not take into account the impacts of repeated exposures. Therefore, we counted them together at the initial analysis and detailed differences in symptoms in Table 2.

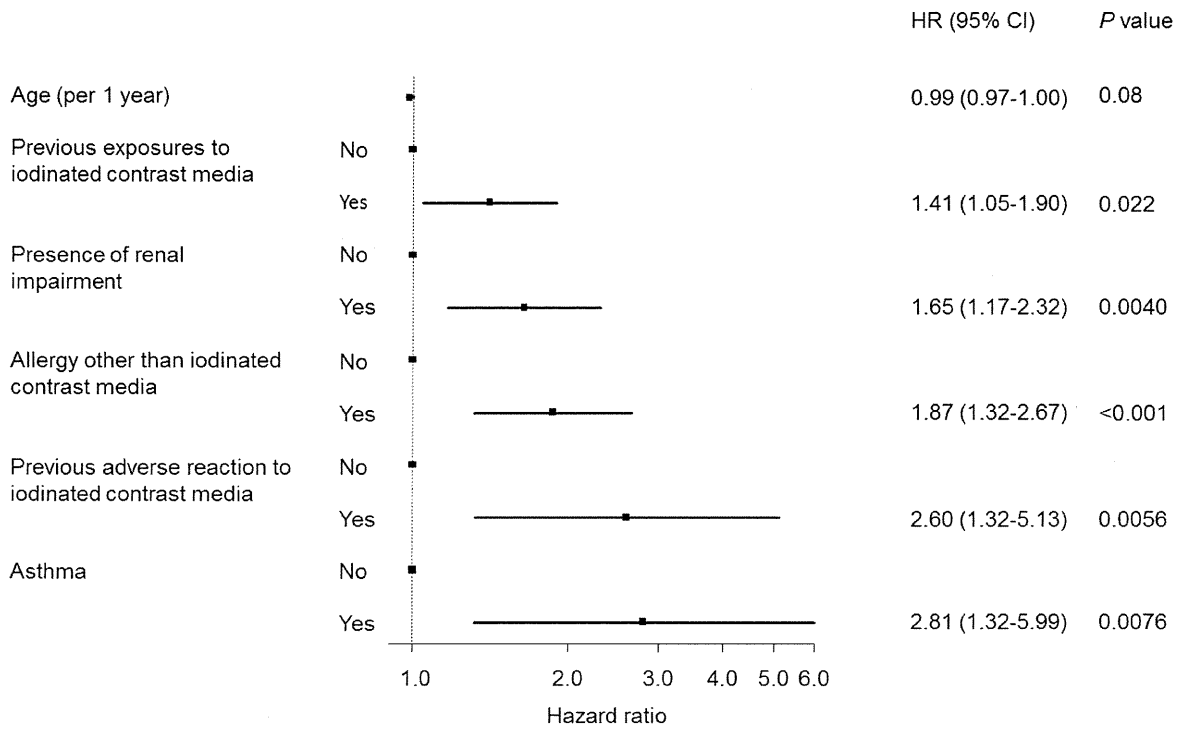

Figure 3. Forest plot of the hazard ratios for an initial adverse reaction during the study period.

doi: 10.1371/journal.pone.0076018.g003

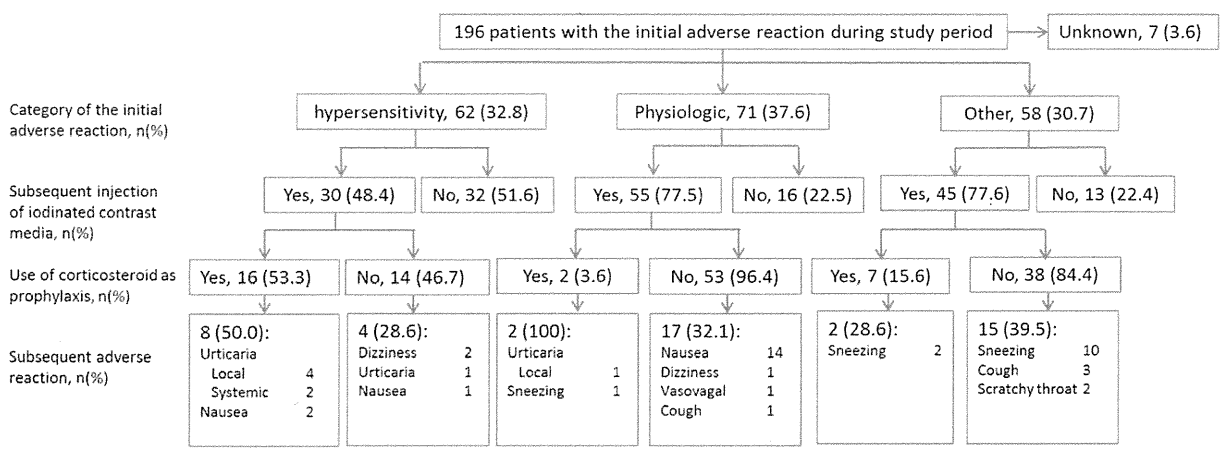

Figure 4. Subsequent contrast media injections and subsequent adverse reaction to iodinated contrast media.

doi: 10.1371/journal.pone.0076018.g004

In conclusion, the risk of immediate AR to iodinated CM increases with repeated exposures, and the incidence is strongly associated with renal function in patients with HCC. Not only renal toxicity but also AR to CM should be monitored carefully when iodinated CM are injected into HCC patients with mild renal impairment. However, even if patients with previous AR for iodinated CM were re-injected with iodinated CM, the patients with HCC had subsequent reactions at levels similar to the initial reaction.

Author Contributions

Conceived and designed the experiments: NF RT. Analyzed the data: NF RT MT. Wrote the manuscript: NF RT HY. Drafted

the article: NF RT MA TM SM MS KU KE YK YA NY TG SS. Critical revisions: RT HY KO KK. Treatment and data collection: NF RT.

References

1. Ferlay J, Shin HR, Bray F, Forman D, Mathers C et al. (2010) Estimates of worldwide burden of cancer in 2008: GLOBOCAN 2008. Int J Cancer 127: 2893-2917. doi:10.1002/ijc.25516. PubMed: 21351269.
2. Bosch FX, Ribes J, Díaz M, Cléries R (2004) Primary liver cancer: worldwide incidence and trends. Gastroenterology 127: S5-S16. doi: 10.1053/j.gastro.2004.05.058. PubMed: 15508102.
3. El-Serag HB (2011) Hepatocellular carcinoma. N Engl J Med 365: 1118-1127. doi:10.1056/NEJMra1001683. PubMed: 21992124.
4. Mikami S, Tateishi R, Akahane M, Asaoka Y, Kondo Y et al. (2012) Computed tomography follow-up for the detection of hepatocellular carcinoma recurrence after initial radiofrequency ablation: a single-center experience. J Vasc Interv Radiol 23: 1269-1275. doi:10.1016/j.jvir.2012.06.032. PubMed: 22999746.
5. Shiina S, Tateishi R, Arano T, Uchino K, Enooku K et al. (2012) Radiofrequency ablation for hepatocellular carcinoma: 10-year outcome and prognostic factors. Am J Gastroenterol 107: 569-577; quiz: 10.1038/ajg.2011.425. PubMed: 22158026.
6. Caro JJ, Trindade E, McGregor M (1991) The risks of death and of severe nonfatal reactions with high- vs low-osmolality contrast media: a meta-analysis. AJR Am J Roentgenol 156: 825-832. doi:10.2214/ajr.156.4.1825900. PubMed: 1825900.
7. Wolf GL, Mishkin MM, Roux SG, Halpern EF, Gottlieb J et al. (1991) Comparison of the rates of adverse drug reactions. Ionic contrast agents, ionic agents combined with steroids, and nonionic agents. Invest Radiol 26: 404-410. doi:10.1097/00004424-199105000-00003. PubMed: 2055736.
8. Hagan JB (2004) Anaphylactoid and adverse reactions to radiocontrast agents. Immunol Allergy Clin North Am 24: 507-519, vii-viii doi:10.1016/j.iac.2004.03.005. PubMed: 15242724.
9. Johansson SG, Bieber T, Dahl R, Friedmann PS, Lanier BQ et al.. (2004) Revised nomenclature for allergy for global use: Report of the Nomenclature Review Committee of the World Allergy Organization, October 2003. J Allergy Clin Immunol 113: 832-836. doi:10.1016/j.jaci.2003.12.591. PubMed: 15131563.
10. Barrett BJ, Parfrey PS, McDonald JR, Hefferton DM, Reddy ER et al. (1992) Nonionic low-osmolality versus ionic high-osmolality contrast material for intravenous use in patients perceived to be at high risk: randomized trial. Radiology 183: 105-110. PubMed: 1549654.
11. Katayama H, Yamaguchi K, Kozuka T, Takashima T, Seez P et al. (1990) Adverse reactions to ionic and nonionic contrast media. A report from the Japanese Committee on the Safety of Contrast Media. Radiology 175: 621-628. PubMed: 2343107.
12. Andrew E, Berg KJ (2004) Nephrotoxic effects of X-ray contrast media. J Toxicol Clin Toxicol 42: 325-332. doi:10.1081/CLT-120037430. PubMed: 15362604.
13. Morcos SK, Thomsen HS (2001) Adverse reactions to iodinated contrast media. Eur Radiol 11: 1267-1275. doi:10.1007/s003300000729. PubMed: 11471623.
14. Levey AS, de Jong PE, Coresh J, El Nahas M, Astor BC et al. (2011) The definition, classification, and prognosis of chronic kidney disease: a KDIGO Controversies Conference report. Kidney Int 80: 17-28. doi: 10.1038/ki.2010.483. PubMed: 21150873.
15. Pugh RN, Murray-Lyon IM, Dawson JL, Pietroni MC, Williams R (1973) Transection of the oesophagus for bleeding oesophageal varices. Br J Surg 60: 646-649. doi:10.1002/bjs.1800600817. PubMed: 4541913.
16. Tramèr MR, von Elm E, Loubeyre P, Hauser C (2006) Pharmacological prevention of serious anaphylactic reactions due to iodinated contrast media: systematic review. BMJ 333: 675. doi:10.1136/bmj.38905.634132.AE. PubMed: 16880193.
17. Lasser EC, Berry CC, Talner LB, Santini LC, Lang EK et al. (1987) Pretreatment with corticosteroids to alleviate reactions to intravenous contrast material. N Engl J Med 317: 845-849. doi:10.1056/NEJM198710013171401. PubMed: 3627208.
18. Greenberger PA, Patterson R, Tapio CM (1985) Prophylaxis against repeated radiocontrast media reactions in 857 cases. Adverse experience with cimetidine and safety of beta-adrenergic antagonists. Arch Intern Med 145: 2197-2200. doi:10.1001/archinte.145.12.2197. PubMed: 2866755.
19. Thomsen HS, Morcos SK (2006) ESUR guidelines on contrast media. Abdom Imaging 31: 131-140. doi:10.1007/s00261-005-0380-y. PubMed: 16447092.
20. Ichikawa T, Saito K, Yoshioka N, Tanimoto A, Gokan T et al. (2010) Detection and characterization of focal liver lesions: a Japanese phase III, multicenter comparison between gadoxetic acid disodium-enhanced magnetic resonance imaging and contrast-enhanced computed tomography predominantly in patients with hepatocellular carcinoma and chronic liver disease. Invest Radiol 45: 133-141. doi:10.1097/RLI.0b013e3181caea5b. PubMed: 20098330.
21. Hwang J, Kim SH, Lee MW, Lee JY (2012) Small (</= 2 cm) hepatocellular carcinoma in patients with chronic liver disease: comparison of gadoxetic acid-enhanced 3.0 T MRI and multiphasic 64-multirow detector CT. British Journal of Radiology 85: e314-322.
22. Lencioni R, Piscaglia F, Bolondi L (2008) Contrast-enhanced ultrasound in the diagnosis of hepatocellular carcinoma. J Hepatol 48: 848-857. doi:10.1016/j.jhep.2008.02.005. PubMed: 18328590.
23. Sano K, Ichikawa T, Motosugi U, Sou H, Muhi AM et al. (2011) Imaging study of early hepatocellular carcinoma: usefulness of gadoxetic acid-enhanced MR imaging. Radiology 261: 834-844. doi:10.1148/radiol.11101840. PubMed: 21998047.
24. Khalili K, Kim TK, Jang HJ, Haider MA, Khan L et al. (2011) Optimization of imaging diagnosis of 1-2 cm hepatocellular carcinoma: an analysis of diagnostic performance and resource utilization. J Hepatol 54: 723-728. doi:10.1016/j.jhep.2010.07.025. PubMed: 21156219.
25. American College of Radiology (2012) Adverse Events After Intravascular Iodinated Contrast Media Administration. ACR Manual on Contrast Media version 8. Reston, VA, American: College of Radiology. pp. 21-28.
26. Greenland S (1995) Dose-response and trend analysis in epidemiology: alternatives to categorical analysis. Epidemiology 6: 356-365. doi:10.1097/00001648-199507000-00005. PubMed: 7548341.
27. Agresti A (2002) Categorical Data Analysis, 2nd ed. New York: Wiley.
28. Levey AS, Eckardt KU, Tsukamoto Y, Levin A, Coresh J et al. (2005) Definition and classification of chronic kidney disease: a position statement from Kidney Disease: Improving Global Outcomes (KDIGO). Kidney Int 67: 2089-2100. doi:10.1111/j.1523-1755.2005.00365.x. PubMed: 15882252.
29. Davenport MS, Cohan RH, Caoili EM, Ellis JH (2009) Repeat contrast medium reactions in premedicated patients: frequency and severity. Radiology 253: 372-379. doi:10.1148/radiol.2532090465. PubMed: 19789241.
30. Freed KS, Leder RA, Alexander C, DeLong DM, Kliewer MA (2001) Breakthrough adverse reactions to low-osmolar contrast media after steroid premedication. AJR Am J Roentgenol 176: 1389-1392. doi: 10.2214/ajr.176.6.1761389. PubMed: 11373198.
31. Lang DM, Alpern MB, Visintainer PF, Smith ST (1991) Increased risk for anaphylactoid reaction from contrast media in patients on beta-adrenergic blockers or with asthma. Ann Intern Med 115: 270-276. doi: 10.7326/0003-4819-115-4-270. PubMed: 1677239.
32. Lang DM, Alpern MB, Visintainer PF, Smith ST (1993) Elevated risk of anaphylactoid reaction from radiographic contrast media is associated with both beta-blocker exposure and cardiovascular disorders. Arch Intern Med 153: 2033-2040. doi:10.1001/archinte.1993.00410170119012. PubMed: 8102844.
33. Bettmann MA, Heeren T, Greenfield A, Goudey C (1997) Adverse events with radiographic contrast agents: results of the SCVIR Contrast Agent Registry. Radiology 203: 611-620. PubMed: 9169677.
34. Dahlstrom K, Shaw DD, Clauss W, Andrew E, Sveen K (1985) Summary of U.S. and European intravascular experience with iohexol based on the clinical trial program. Invest Radiol 20: S117-S121. doi: 10.1097/00004424-198501002-00028. PubMed: 3882613.
35. Kopp AF, Mortele KJ, Cho YD, Palkowitsch P, Bettmann MA et al. (2008) Prevalence of acute reactions to iopromide: postmarketing surveillance study of 74,717 patients. Acta Radiol 49: 902-911. doi: 10.1080/02841850802282811. PubMed: 18651252.

Cell

Identification of Liver Cancer Progenitors Whose Malignant Progression Depends on Autocrine IL-6 Signaling

Guobin He,[1,13] Debanjan Dhar,[1,13] Hayato Nakagawa,[1,11,13] Joan Font-Burgada,[1,13] Hisanobu Ogata,[1,12,13] Yuhong Jiang,[1] Shabnam Shalapour,[1] Ekihiro Seki,[2] Shawn E. Yost,[4,5] Kristen Jepsen,[5] Kelly A. Frazer,[5,6,7,8] Olivier Harismendy,[5,6,7] Maria Hatziapostolou,[9] Dimitrios Iliopoulos,[9] Atsushi Suetsugu,[3,10] Robert M. Hoffman,[3,10] Ryosuke Tateishi,[11] Kazuhiko Koike,[11] and Michael Karin[1,6,*]

[1]Laboratory of Gene Regulation and Signal Transduction, Departments of Pharmacology and Pathology
[2]Department of Medicine
[3]Department of Surgery
[4]Bioinformatics Graduate Program
[5]Rady's Children's Hospital and Department of Pediatrics
[6]Moores UCSD Cancer Center
[7]Clinical and Translational Research Institute
[8]Institute for Genomic Medicine
University of California San Diego, School of Medicine, 9500 Gilman Drive, San Diego, CA 92093, USA
[9]Center for Systems Biomedicine, Division of Digestive Diseases and Institute for Molecular Medicine, David Geffen School of Medicine, University of California Los Angeles, Los Angeles, CA 90095, USA
[10]AntiCancer, Inc., San Diego, CA 92111, USA
[11]Department of Gastroenterology, University of Tokyo, Tokyo 113-8655, Japan
[12]Department of Medicine and Clinical Science, Graduate School of Medical Sciences, Kyushu University, Fukuoka 812-8582, Japan
[13]These authors contributed equally to this work
*Correspondence: karinoffice@ucsd.edu
http://dx.doi.org/10.1016/j.cell.2013.09.031

SUMMARY

Hepatocellular carcinoma (HCC) is a slowly developing malignancy postulated to evolve from premalignant lesions in chronically damaged livers. However, it was never established that premalignant lesions actually contain tumor progenitors that give rise to cancer. Here, we describe isolation and characterization of HCC progenitor cells (HcPCs) from different mouse HCC models. Unlike fully malignant HCC, HcPCs give rise to cancer only when introduced into a liver undergoing chronic damage and compensatory proliferation. Although HcPCs exhibit a similar transcriptomic profile to bipotential hepatobiliary progenitors, the latter do not give rise to tumors. Cells resembling HcPCs reside within dysplastic lesions that appear several months before HCC nodules. Unlike early hepatocarcinogenesis, which depends on paracrine IL-6 production by inflammatory cells, due to upregulation of LIN28 expression, HcPCs had acquired autocrine IL-6 signaling that stimulates their in vivo growth and malignant progression. This may be a general mechanism that drives other IL-6-producing malignancies.

INTRODUCTION

Every malignant tumor is probably derived from a single progenitor that had acquired growth and survival advantages through genetic and epigenetic changes, allowing clonal expansion (Nowell, 1976). Tumor progenitors are not necessarily identical to cancer stem cells (CSCs), which maintain and renew fully established malignancies (Nguyen et al., 2012). However, clonal evolution and selective pressure may cause some descendants of the initial progenitor to cross the bridge of no return and form a premalignant lesion. Cancer genome sequencing indicates that most cancers require at least five genetic changes to evolve (Wood et al., 2007). How these changes affect the properties of tumor progenitors and control their evolution into a CSC is not entirely clear, as it has been difficult to isolate and propagate cancer progenitors prior to detection of tumor masses. Given these difficulties, it is also not clear whether cancer progenitors are the precursors for the more malignant CSC isolated from fully established cancers. An answer to these critical questions depends on identification and isolation of cancer progenitors, which may also enable definition of molecular markers and signaling pathways suitable for early detection and treatment. This is especially important in cancers of the liver and pancreas, which evolve over the course of many years but, once detected, are extremely difficult to treat (El-Serag, 2011; Hruban et al., 2007).

Hepatocellular carcinoma (HCC), the most common liver cancer, is the end product of chronic liver diseases, requiring

several decades to evolve (El-Serag, 2011). Currently, HCC is the third most deadly and fifth most common cancer worldwide, and in the United States its incidence has doubled in the past two decades. Furthermore, 8% of the world's population are chronically infected with hepatitis B or C viruses (HBV and HCV) and are at a high risk of new HCC development (El-Serag, 2011). Up to 5% of HCV patients will develop HCC in their lifetime, and the yearly HCC incidence in patients with cirrhosis is 3%–5%. These tumors may arise from premalignant lesions, ranging from dysplastic foci to dysplastic hepatocyte nodules that are often seen in damaged and cirrhotic livers and are more proliferative than the surrounding parenchyma (Hytiroglou et al., 2007). However, the tumorigenic potential of these lesions was never examined, and it is unknown whether they contain any genetic alterations. Given that there is no effective treatment for HCC and, upon diagnosis, most patients with advanced disease have a remaining lifespan of 4–6 months, it is important to detect HCC early, while it is still amenable to surgical resection or chemotherapy. Premalignant lesions, called foci of altered hepatocytes (FAH), were also described in chemically induced HCC models (Pitot, 1990), but it was questioned whether these lesions harbor tumor progenitors or result from compensatory proliferation (Sell and Leffert, 2008). The aim of this study was to determine whether HCC progenitor cells (HcPCs) exist and if so, to isolate these cells and identify some of the signaling networks that are involved in their maintenance and progression.

We now describe HcPC isolation from mice treated with the procarcinogen diethyl nitrosamine (DEN), which induces poorly differentiated HCC nodules within 8 to 9 months (Verna et al., 1996). Although these tumors do not evolve in the context of cirrhosis, the use of a chemical carcinogen is justified because the finding of up to 121 mutations per HCC genome suggests that carcinogens may be responsible for human HCC induction (Guichard et al., 2012). Furthermore, 20%–30% of HCC, especially in HBV-infected individuals, evolve in noncirrhotic livers (El-Serag, 2011). Nonetheless, we also isolated HcPCs from *Tak1*$^{\Delta hep}$ mice, which develop spontaneous HCC as a result of progressive liver damage, inflammation, and fibrosis caused by ablation of TAK1 (Inokuchi et al., 2010). Although the etiology of each model is distinct, both contain HcPCs that express marker genes and signaling pathways previously identified in human HCC stem cells (Marquardt and Thorgeirsson, 2010) long before visible tumors are detected. Furthermore, DEN-induced premalignant lesions and HcPCs exhibit autocrine IL-6 production that is critical for tumorigenic progression. Circulating IL-6 is a risk indicator in several human pathologies and is strongly correlated with adverse prognosis in HCC and cholangiocarcinoma (Porta et al., 2008; Soresi et al., 2006). IL-6 produced by in-vitro-induced CSCs was suggested to be important for their maintenance (Iliopoulos et al., 2009). Furthermore, autocrine IL-6 was detected in several cancers, but its origin is poorly understood (Grivennikov and Karin, 2008). In particular, little is known about the source of IL-6 in HCC. In early stages of hepatocarcinogenesis, IL-6 is produced by Kupffer cells or macrophages (Maeda et al., 2005; Naugler et al., 2007). However, paracrine IL-6 production is transient and does not explain its expression by HCC cells.

RESULTS

DEN-Induced Collagenase-Resistant Aggregates of HCC Progenitors

A single intraperitoneal (i.p.) injection of DEN into 15-day-old BL/6 mice induces HCC nodules first detected 8 to 9 months later. However, hepatocytes prepared from macroscopically normal livers 3 months after DEN administration already contain cells that progress to HCC when transplanted into the permissive liver environment of MUP-uPA mice (He et al., 2010), which express urokinase plasminogen activator (uPA) from a mouse liver-specific major urinary protein (MUP) promoter and undergo chronic liver damage and compensatory proliferation (Rhim et al., 1994). Collagenase digestion of DEN-treated livers generated a mixture of monodisperse hepatocytes and aggregates of tightly packed small hepatocytic cells (Figure 1A). Aggregated cells were also present—but in lower abundance—in digests of control livers (Figure S1A available online). HCC markers such as α fetoprotein (AFP), glypican 3 (Gpc3), and Ly6D, whose expression in mouse liver cancer was reported (Meyer et al., 2003), were upregulated in aggregates from DEN-treated livers, but not in nonaggregated hepatocytes or aggregates from control livers (Figure S1A). Thus, control liver aggregates may result from incomplete collagenase digestion, whereas aggregates from DEN-treated livers may contain HcPC. DEN-induced aggregates became larger and more abundant 5 months after carcinogen exposure, when they consisted of 10–50 cells that were smaller than nonaggregated hepatocytes. Using 70 μm and 40 μm sieves, we separated aggregated from nonaggregated hepatocytes (Figure 1A) and tested their tumorigenic potential by transplantation into MUP-uPA mice (Figure 1B). To facilitate transplantation, the aggregates were mechanically dispersed and suspended in Dulbecco's modified Eagle's medium (DMEM). Five months after intrasplenic (i.s.) injection of 10^4 viable cells, mice receiving cells from aggregates developed about 18 liver tumors per mouse, whereas mice receiving nonaggregated hepatocytes developed less than 1 tumor each (Figure 1B). The tumors exhibited typical trabecular HCC morphology and contained cells that abundantly express AFP (Figure S1B). To confirm that the HCCs were derived from transplanted cells, we measured their relative MUP-uPA DNA copy number and found that they contained much less MUP-uPA transgene DNA than the surrounding parenchyma (Figure S1C). Transplantation of aggregated cells from livers of DEN-treated actin-GFP transgenic mice resulted in GFP-positive HCCs (Figure S1D). Both experiments strongly suggest that the HCCs were derived from the transplanted cells. No tumors were ever observed after transplantation of control hepatocytes (nonaggregated or aggregated).

Only liver tumors were formed by the transplanted cells. Other organs, including the spleen into which the cells were injected, remained tumor free (Figure 1B), suggesting that HcPCs progress to cancer only in the proper microenvironment. Indeed, no tumors appeared after HcPC transplantation into normal BL/6 mice. But, if BL/6 mice were first treated with retrorsine (a chemical that permanently inhibits hepatocyte proliferation [Laconi et al., 1998]), intrasplenically transplanted with HcPC-containing aggregates, and challenged with CCl_4 to induce liver injury and compensatory proliferation (Guo et al., 2002), HCCs readily

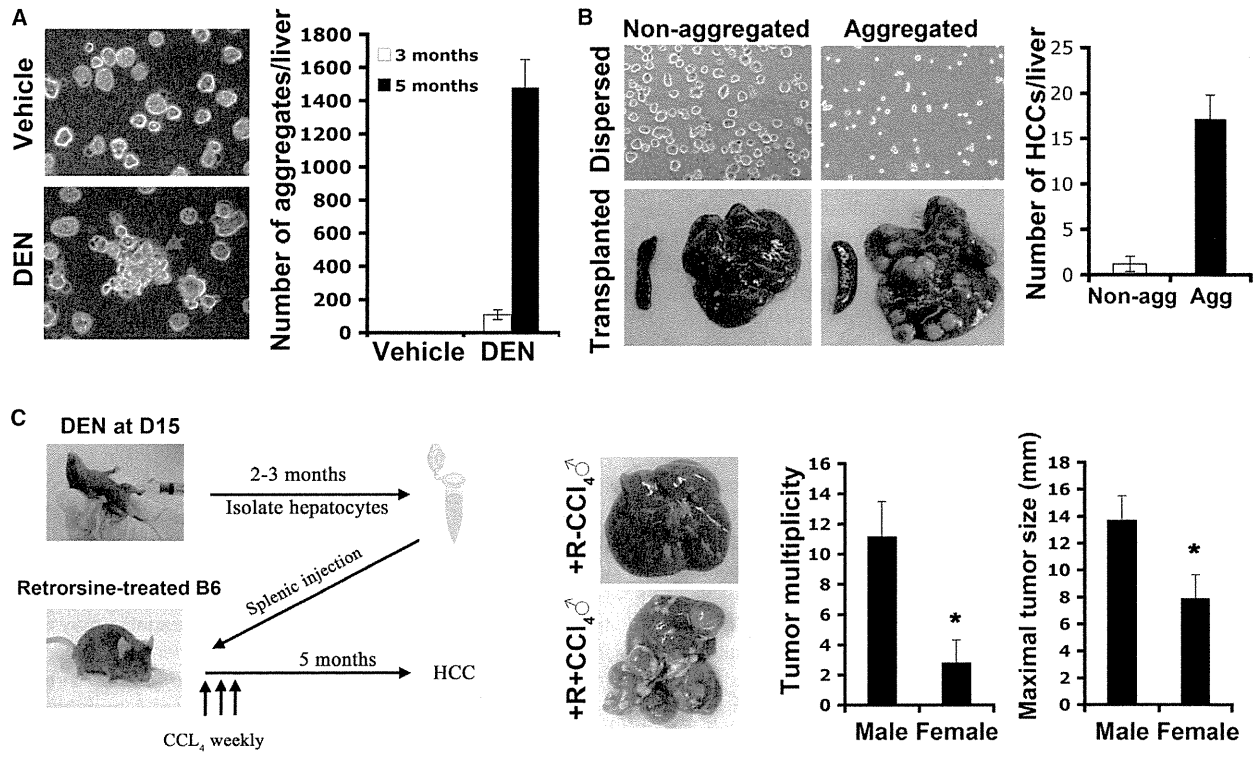

E

Type of cells	Number of cells transplanted			
	$4x10^4$	$1X10^4$	1000	100
Unsorted	2(2)	9(9)	2(5)	0(3)
$CD44^+$	nd	nd	4(4)	2(4)
$CD44^-$	nd	nd	0(4)	0(5)

Figure 1. DEN-Induced Hepatocytic Aggregates Contain $CD44^+$ HCC Progenitors

(A) Fifteen-day-old BL/6 males were given DEN or vehicle. After 3 or 5 months, their livers were removed and collagenase digested. Left: typical digest appearance (magnification: 400×; 3 months after DEN). Red arrow indicates a collagenase-resistant aggregate. Right: aggregates per liver (n = 5; ± SD for each point).

(B) Livers were collagenase digested 5 months after DEN administration. Aggregates were separated from nonaggregated cells and mechanically dispersed into a single-cell suspension (left upper panels; 200×). 10^4 viable aggregated or nonaggregated cells were i.s. injected into MUP-uPA mice whose livers and spleens were analyzed for tumors 5 months later (left lower panels). The number of HCC nodules per liver was determined (n = 5; ± SD).

(C) Adult BL/6 mice were given retrorsine twice with a 2 week interval to inhibit hepatocyte proliferation. After 1 month, mice were i.s. transplanted with dispersed hepatocyte aggregates (10^4 cells) from DEN-treated mice and, 2 weeks later, were given three weekly i.p. injections of CCl_4 or vehicle. Tumor multiplicity and size were evaluated 5 months later (n = 5; ± SD).

(D) Hepatocyte aggregates were prepared as in (A), stained with CD44 antibody and DAPI, and examined by fluorescent microscopy (400×).

(E) Hepatocyte aggregates were dispersed as above, and $CD44^+$ cells were separated from $CD44^-$ cells. The indicated cell numbers were injected into MUP-uPA mice, and HCC development was evaluated 5 months later. n values are in parentheses (n.d., not done).

See also Figure S1.

appeared (Figure 1C). CCl_4 omission prevented tumor development. Notably, MUP-uPA or CCl_4-treated livers are fragile, rendering direct intrahepatic transplantation difficult. The transplanted HcPC-containing aggregates formed more numerous and larger HCC nodules in male recipients than in females (Figure 1C), as observed in MUP-uPA mice transplanted with unfractionated DEN-exposed hepatocytes (He et al., 2010). Thus, CCl_4-induced liver damage, especially within a male liver, generates a microenvironment that drives HcPC proliferation and malignant progression. To examine this point, we transplanted GFP-labeled HcPC-containing aggregates into retrorsine-treated BL/6 mice and examined their ability to proliferate with or without subsequent CCl_4 treatment. Indeed, the GFP^+ cells formed clusters that grew in size only in CCl_4-treated host livers

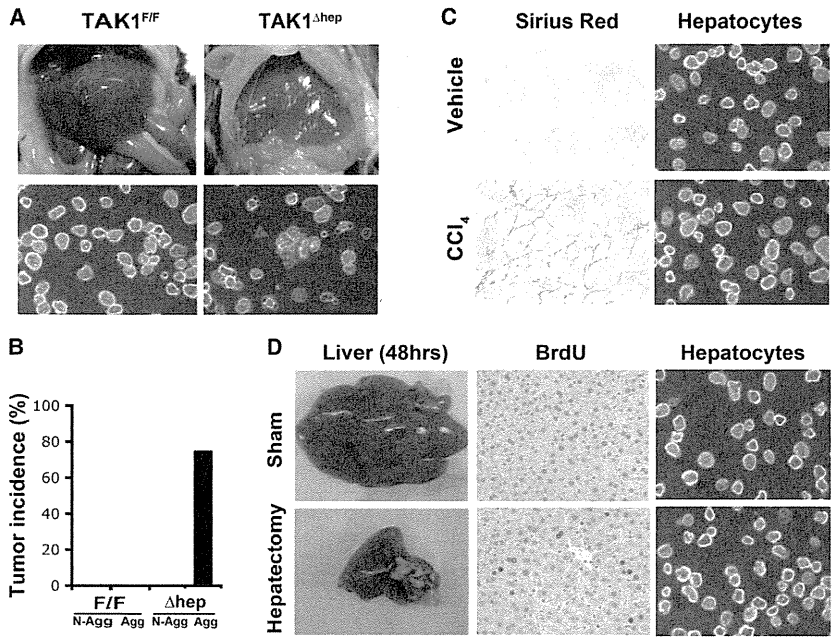

Figure 2. *Tak1*$^{\Delta hep}$ Livers Contain Collagenase-Resistant HcPC Aggregates

(A) Livers, free of tumors (upper panels), were removed from 1-month-old *Tak1*$^{F/F}$ and *Tak1*$^{\Delta hep}$ males and collagenase digested (lower panels; red arrow indicates collagenase-resistant aggregate).

(B) 10^4 nonaggregated or dispersed aggregated hepatocytes from (A) were i.s. injected into MUP-uPA mice that were analyzed 6 months later to identify mice with at least one liver tumor (n = 5–8 mice per genotype).

(C) BL/6 males were injected with vehicle or CCl_4 twice weekly for 2 weeks. Hepatocytes were isolated by collagenase digestion and photographed (right panels; 400×). Liver sections were stained with Sirius red to reveal collagen deposits (left panels).

(D) 8-week-old BL/6 males were subjected to 70% partial hepatectomy, pulsed with BrdU at 46 and 70 hr, and sacrificed 2 hr later. Isolated hepatocytes were photographed. Liver sections were analyzed for BrdU incorporation (400×). See also Figure S2 and Table S1.

(Figure S1E). Omission of $CC1_4$ prevented their expansion. Unlike HCC-derived cancer cells (dih10 cells), which form subcutaneous (s.c.) tumors with HCC morphology (He et al., 2010; Park et al., 2010), the HcPC-containing aggregates did not generate s.c. tumors in BL/6 mice (Figure S1F).

Despite their homogeneous appearance, the HcPC-containing aggregates contained both $CD44^+$ and $CD44^-$ cells (Figure 1D). Because CD44 is expressed by HCC stem cells (Yang et al., 2008; Zhu et al., 2010), we dispersed the aggregates and separated $CD44^+$ from $CD44^-$ cells and transplanted both into MUP-uPA mice. Whereas as few as 10^3 $CD44^+$ cells gave rise to HCCs in 100% of recipients, no tumors were detected after transplantation of $CD44^-$ cells (Figure 1E). Remarkably, 50% of recipients developed at least one HCC after receiving as few as 10^2 $CD44^+$ cells. Mature $CD44^-$ hepatocytes were found to engraft as well as or better than $CD44^+$ small hepatocytic cells (Haridass et al., 2009; Ichinohe et al., 2012). Hence, livers of DEN-treated mice contain $CD44^+$ HcPC that can be successfully isolated and purified and give rise to HCCs after transplantation into appropriate hosts. Unlike fully transformed HCC cells, HcPCs only give rise to tumors within the liver.

HcPC-Containing Aggregates in *Tak1*$^{\Delta hep}$ Mice

We applied the same HcPC isolation protocol to *Tak1*$^{\Delta hep}$ mice, which develop HCC of different etiology from DEN-induced HCC. Importantly, *Tak1*$^{\Delta hep}$ mice develop HCC as a consequence of chronic liver injury and fibrosis without carcinogen or toxicant exposure (Inokuchi et al., 2010). Indeed, whole-tumor exome sequencing revealed that DEN-induced HCC contained about 24 mutations per 10^6 bases (Mb) sequenced, with *B-Raf*^{V637E} being the most recurrent, whereas 1.4 mutations per Mb were detected in *Tak1*$^{\Delta hep}$ HCC's exome (Table S1). By contrast, *Tak1*$^{\Delta hep}$ HCC exhibited gene copy number changes.

Collagenase digests of 1-month-old *Tak1*$^{\Delta hep}$ livers contained much more hepatocytic aggregates than *Tak1*$^{f/f}$ liver digests (Figure 2A). Notably, HCC developed in 75% of MUP-uPA mice that received dispersed *Tak1*$^{\Delta hep}$ aggregates, but no tumors appeared in mice receiving nonaggregated *Tak1*$^{\Delta hep}$ or total *Tak1*$^{f/f}$ hepatocytes (Figure 2B). Because *Tak1*$^{\Delta hep}$ mice are subject to chronic liver damage and consequent compensatory proliferation, we wanted to ascertain that the HcPCs are not simply proliferating hepatocytes or expanding bipotential hepatobiliary progenitors using CCl_4 to induce liver injury and compensatory proliferation in WT mice. Although this treatment caused acute liver fibrosis, it did not augment formation of collagenase-resistant aggregates (Figure 2C). Similarly, few aggregates were detected in collagenase digests of livers after partial hepatectomy (Figure 2D). However, bile duct ligation (BDL) or feeding with 3,5-dicarbethoxy-1,4-dihydrocollidine (DDC), treatments that cause cholestatic liver injuries and oval cell expansion (Dorrell et al., 2011), did increase the number of small hepatocytic cell aggregates (Figure S2A). Nonetheless, no tumors were observed 5 months after injection of such aggregates into MUP-uPA mice (Figure S2B). Thus, not all hepatocytic aggregates contain HcPCs, and HcPCs only appear under tumorigenic conditions.

The HcPC Transcriptome Is Similar to that of HCC and Oval Cells

To determine the relationship between DEN-induced HcPCs, normal hepatocytes, and fully transformed HCC cells, we analyzed the transcriptomes of aggregated and nonaggregated hepatocytes from male littermates 5 months after DEN administration, HCC epithelial cells from DEN-induced tumors, and normal hepatocytes from age- and gender-matched littermate controls. Clustering analysis distinguished the HCC samples from other samples and revealed that the aggregated

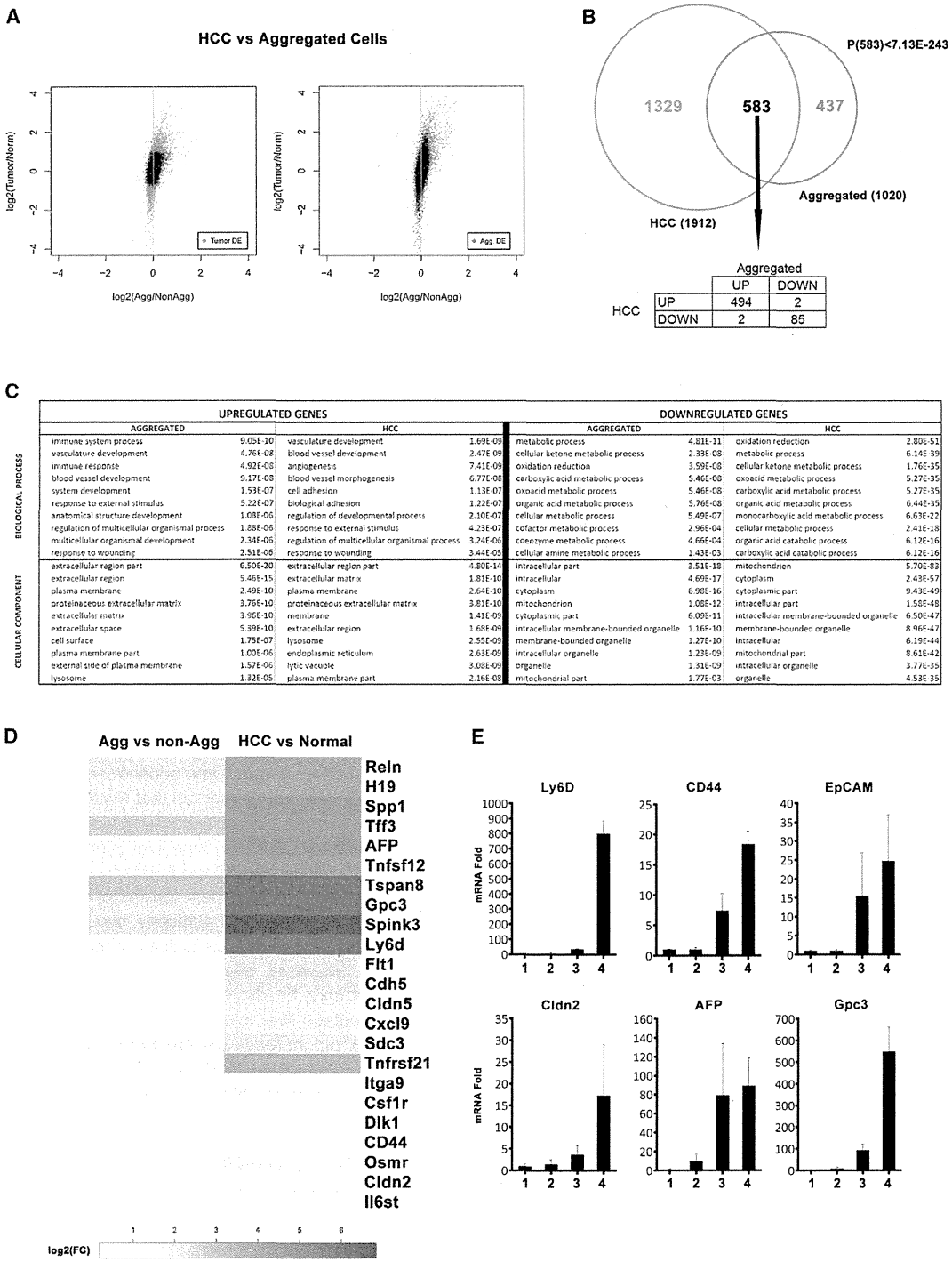

Figure 3. Aggregated Hepatocytes Exhibit an Altered Transcriptome Similar to that of HCC Cells

Aggregated and matched nonaggregated hepatocytes were isolated 5 months after DEN treatment. HCC cells were isolated from DEN-induced tumors, and normal hepatocytes were from age- and gender-matched control mice. RNA was extracted and subjected to microarray analysis (n = 3 for each sample).

(A) Scatterplot representing fold changes (log 2 of expression ratio) in gene expression for HCC versus normal (y axis) and aggregated versus nonaggregated (x axis) pairwise transcriptome comparisons. The plot is displayed twice: in the left panel, genes with an FDR < 0.01 in the aggregated versus nonaggregated

(legend continued on next page)

hepatocyte samples did not cluster with each other but rather with nonaggregated hepatocytes derived from the same mouse (Figure S3A). Interestingly, the aggregated cell transcriptome appeared closer to that of normal hepatocytes than to the HCC profile. This similarity may be due to the presence of ~70% nontumorigenic (or $CD44^-$) hepatocytes within the purified aggregates (Figure 1D). Comparison of the HCC and normal hepatocyte transcriptomes revealed 1,912 differentially expressed genes (false discovery rate [FDR] < 0.01; Figure 3A, left, cyan dots). A similar comparison revealed 1,020 genes that are differentially expressed between aggregated and nonaggregated hepatocytes (FDR < 0.01; Figure 3A, right, red dots). The range of differential expression is wider for the HCC and normal hepatocyte pair than the aggregate versus nonaggregate pair, reflecting presence of normal, nontransformed hepatocytes within the aggregates, resulting in signal dilution. Interestingly, 57% (583/1,020) of genes differentially expressed in aggregated relative to nonaggregated hepatocytes are also differentially expressed in HCC relative to normal hepatocytes (Figure 3B, top), a value that is highly significant ($p < 7.13 \times 10^{-243}$). More specifically, 85% (494/583) of these genes are overexpressed in both HCC and HcPC-containing aggregates (Figure 3B, bottom table). Thus, hepatocyte aggregates isolated 5 months after DEN injection contain cells that are related in their gene expression profile to HCC cells isolated from fully developed tumor nodules.

To gain insight into the functional differences between the transcriptomes of the four populations, we examined which biological processes or cellular compartments were significantly overrepresented in the induced or repressed genes in both pairwise comparisons (Gene Ontology Analysis). As expected, processes and compartments that were enriched in aggregated hepatocytes relative to nonaggregated hepatocytes were almost identical to those that were enriched in HCC relative to normal hepatocytes (Figure 3C). Upregulated genes were related to immune response, angiogenesis, development, and wound healing, and many encoded plasma membrane or secreted proteins. By contrast, downregulated genes were highly enriched for metabolic processes, and many of them encoded mitochondrial proteins or had functions associated with differentiated hepatocytes (Figure 3C). Several human HCC markers, including AFP, Gpc3 and H19, were upregulated in aggregated hepatocytes (Figures 3D and 3E). Aggregated hepatocytes also expressed more Tetraspanin 8 (Tspan8), a cell-surface glycoprotein that complexes with integrins and is overexpressed in human carcinomas (Zöller, 2009). Another cell-surface molecule highly expressed in aggregated cells is Ly6D (Figures 3D and 3E). Immunofluorescence (IF) analysis revealed that Ly6D was undetectable in normal liver but was elevated in FAH and ubiquitously expressed in most HCC cells (Figure S3C). A fluorescent-labeled Ly6D antibody injected into HCC-bearing mice specifically stained tumor nodules (Figure S3D). Other cell-surface molecules that were upregulated in aggregated cells included syndecan 3 (Sdc3), integrin α 9 (Itga9), claudin 5 (Cldn5), and cadherin 5 (Cdh5) (Figure 3D). Aggregated hepatocytes also exhibited elevated expression of extracellular matrix proteins (TIF3 and Reln1) and a serine protease inhibitor (Spink3). Elevated expression of such proteins may explain aggregate formation. Aggregated hepatocytes also expressed progenitor cell markers, including the epithelial cell adhesion molecule (EpCAM) (Figure 3E) and Dlk1 (Figure 3D). Elevated expression of cytokines and cytokine receptors was also detected, including tumor necrosis factor superfamily members 12 and 21, colony-stimulating factor 1 receptor, FMS-like tyrosine kinase 1, chemokine (C-X-C motif) ligand 9, the STAT3-activating cytokine osteopontin, IL-6 receptor (IL-6R) signal transducing subunit (gp130), and oncostatin M (OSM) receptor, which also activates STAT3 (Figure 3D).

Aggregated hepatocytes expressed albumin, albeit less than nonaggregated hepatocytes (Figure 4A). Some aggregated cells were positive for cytokeratin 19 (CK19) and A6, markers for bile duct epithelium and oval cells (Figure 4A). Most cells in the DEN-induced aggregates were AFP positive, and some of them expressed EpCAM (Figure 4A). However, not all markers were expressed by every cell within a given aggregate, suggesting that the aggregates contain liver cells that are related to bipotential hepatobiliary progenitors/oval cells as well as more differentiated progeny and normal hepatocytes. To confirm these observations, we compared the HcPC and HCC (Figure 3A) to the transcriptome of DDC-induced oval cells (Shin et al., 2011). This analysis revealed a striking similarity between the HCC, HcPC, and the oval cell transcriptomes (Figure S3B). Despite these similarities, some genes that were upregulated in HcPC-containing aggregates and HCC were not upregulated in oval cells. Such genes may account for the tumorigenic properties of HcPC and HCC.

We examined the aggregates for signaling pathways and transcription factors involved in hepatocarcinogenesis. Many aggregated cells were positive for phosphorylated c-Jun and STAT3 (Figure 4A), transcription factors involved in DEN-induced

comparison are highlighted in red, and in the right panel, genes with an FDR < 0.01 in the HCC versus normal comparison are highlighted in cyan. DE, differentially expressed.

(B) Venn diagram showing overlap between genes that are differentially expressed between aggregated and nonaggregated hepatocytes and between HCC cells and normal hepatocytes with an FDR < 0.01 (cyan and red dots from A). The probability to find 583 overlapping genes is $<7.13 \times 10^{-243}$. From these 583 common genes, only 4 behaved differently.

(C) The ten most enriched biological processes (upper table) and cellular compartments (lower panel) represented by genes that are significantly upregulated (left panel) or downregulated (right panel) in HCC relative to normal hepatocytes (HCC) or in aggregated relative to nonaggregated hepatocytes (aggregated).

(D) Heatmap displaying positive fold changes (FC) in expression of genes of interest in aggregated versus nonaggregated HcPCs (left) and in HCC versus normal hepatocytes (right).

(E) Expression of selected genes was examined by real-time PCR and is depicted as fold change relative to normal hepatocytes given an arbitrary value of 1.0 (n = 3; ± SD). (1) Normal hepatocytes; (2) nonaggregated hepatocytes from DEN-treated liver; (3) HcPC aggregates from DEN-treated liver; and (4) DEN-induced HCCs.

See also Figure S3.

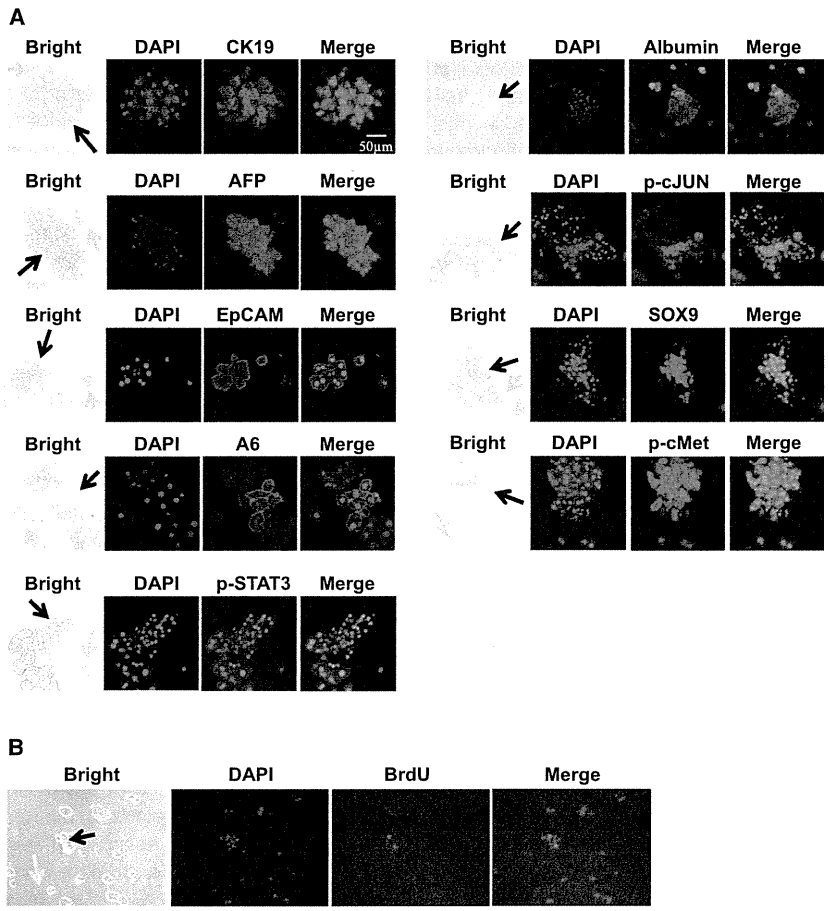

Figure 4. DEN-Induced HcPC Aggregates Express Pathways and Markers Characteristic of HCC and Hepatobiliary Stem Cells

(A) Cytospin preps of collagenase-resistant aggregates from 5-month-old DEN-injected mice were stained with antibodies to CK19, AFP, EpCAM, A6, phospho-Y-STAT3 (Tyr705), albumin, phospho-c-Jun, Sox9, and phospho-c-Met. Black arrows indicate aggregates, and yellow arrows indicate nonaggregated cells (magnification: 400×).

(B) 5-month-old DEN-treated mice were injected with BrdU, and 2 hr later, collagenase-resistant aggregates were isolated and analyzed for BrdU incorporation (400×).

See also Figure S4.

hepatocarcinogenesis (Eferl et al., 2003; He et al., 2010). Sox9, a transcription factor that marks hepatobiliary progenitors (Dorrell et al., 2011), was also expressed by many of the aggregated cells, which were also positive for phosphorylated c-Met (Figure 4A), a receptor tyrosine kinase that is activated by hepatocyte growth factor (HGF) and is essential for liver development (Bladt et al., 1995) and hepatocarcinogenesis (Wang et al., 2001). Few of the nonaggregated hepatocytes exhibited activation of these signaling pathways. Aggregates from bromodeoxyuridine (BrdU)-pulsed DEN-treated mice contained BrdU-positive cells (Figure 4B), indicating that they were actively proliferating prior to isolation. Hepatocyte aggregates from 1-month-old *Tak1*$^{\Delta hep}$ mice also contained cells positive for AFP, Sox9, phosphorylated c-Met, and EpCAM, but not A6-positive cells (Figure S4A). Many of the cells also exhibited partially activated β-catenin, phosphorylated STAT3, and phosphorylated c-Jun. Thus, despite different etiology, HcPC-containing aggregates from *Tak1*$^{\Delta hep}$ mice exhibit upregulation of many of the same markers and pathways that are upregulated in DEN-induced HcPC-containing aggregates. Flow cytometry confirmed enrichment of CD44$^+$ cells as well as CD44$^+$/CD90$^+$ and CD44$^+$/EpCAM$^+$ double-positive cells in the HcPC-containing aggregates from either DEN-treated or *Tak1*$^{\Delta hep}$ livers (Figure S4B).

HcPC-Containing Aggregates Originate from Premalignant Dysplastic Lesions

FAH are dysplastic lesions occurring in rodent livers exposed to hepatic carcinogens (Su et al., 1990). Similar lesions are present in premalignant human livers (Su et al., 1997). Yet, it is still debated whether FAH correspond to premalignant lesions or are a reaction to liver injury that does not lead to cancer (Sell and Leffert, 2008). In DEN-treated males, FAH were detected as early as 3 months after DEN administration (Figure 5A), concomitant with the time at which HcPC-containing aggregates were detected. In females, FAH development was delayed. In both genders, FAH were confined to zone 3 and consisted of tightly packed small hepatocytic cells, some of which were proliferative based on BrdU incorporation (Figure 5B). BrdU$^+$ cells were first detected in DEN-treated males and were confined to FAH and rarely detected in age-matched control mice. FAH contained cells positive for the same progenitor cell markers and activated signaling pathways present in HcPC-containing aggregates, including AFP, CD44, and EpCAM (Figure 5C). FAH also contained cells positive for activated STAT3, c-Jun, and PCNA (Figure 5C). Many cells within FAH exhibited strong upregulation of YAP (Figure 5C), a transcriptional coactivator that is negatively regulated by the Hippo pathway and a liver cancer oncoprotein (Zheng et al., 2011). FAH were also enriched in F4/80$^+$ macrophages (Figure 5C). These results suggest that the HcPC-containing aggregates may be derived from FAH.

HcPCs Exhibit Autocrine IL-6 Expression Necessary for HCC Progression

In situ hybridization (ISH) and immunohistochemistry (IHC) revealed that DEN-induced FAH contained IL-6-expressing cells (Figures 6A, 6B, and S5), and freshly isolated DEN-induced aggregates contained more IL-6 messenger RNA (mRNA) than nonaggregated hepatocytes (Figure 6C). We examined several

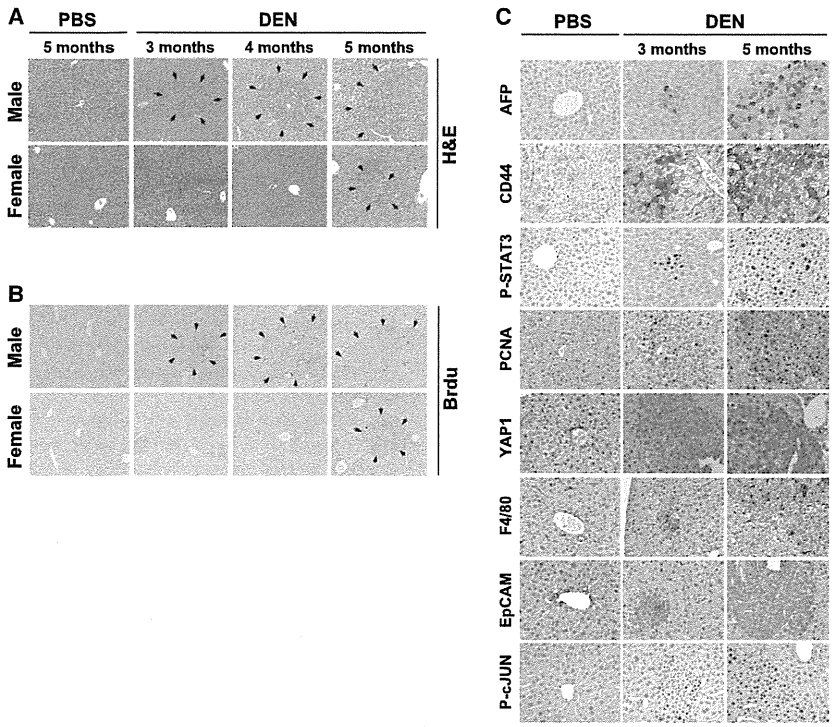

Figure 5. HcPC-Containing Aggregates May Originate from Liver Premalignant Lesions

(A and B) Male and female mice were injected with PBS or DEN at 15 days. At the indicated time points, BrdU was administrated, and livers were collected 2 hr later and stained with H&E (A) or a BrdU-specific antibody (B). Arrows indicate borders of FAH (magnification: 200×).

(C) Sections of male livers treated as above were subjected to IHC with the indicated antibodies (400×).

factors that control IL-6 expression and found that LIN28A and B were significantly upregulated in HcPCs and HCC (Figures 6D and 6E). LIN28-expressing cells were also detected within FAH (Figure 6F). As reported (Iliopoulos et al., 2009), knockdown of LIN28B in cultured HcPC or HCC cell lines decreased IL-6 expression (Figure 6G). LIN28 exerts its effects through downregulation of the microRNA (miRNA) Let-7 (Iliopoulos et al., 2009). Accordingly, miRNA array analysis of aggregated and nonaggregated hepatocytes from DEN-treated mice indicated that the amount of Let-7, along with other miRNAs that also inhibit IL-6 expression (miR194 and miR872), was lower in aggregated cells than in nonaggregated cells (Table S2).

To determine whether autocrine IL-6 production is needed for HCC growth, we silenced IL-6 expression with small hairpin RNA (shRNA) in dih10 HCC cells (He et al., 2010). This resulted in nearly a 75% decrease in IL-6 mRNA (Figure 7A) but had little effect on cell growth in the presence of growth factors, including EGF and insulin (Figure S6A). IL-6 mRNA silencing, however, diminished the ability of dih10 cells to form s.c. tumors (Figures S6B and S6C) and inhibited their ability to form HCCs and proliferate after transplantation into MUP-uPA mice (Figures 7B and S6D). To investigate the importance of autocrine IL-6 production at an earlier step, we isolated HcPC from DEN-treated WT and *Il6*$^{-/-}$ mice. Although IL-6 ablation attenuates HCC induction (Naugler et al., 2007), we still could isolate collagenase-resistant aggregates from livers of DEN-injected *Il6*$^{-/-}$ mice. Notably, IL-6 ablation did not reduce the proportion of CD44^{+} cells in the aggregates (Figures S7A and S7B). We introduced an identical number of WT and *Il6*$^{-/-}$ aggregated hepatocytes into MUP-uPA mice and scored HCC development 5 months later. The IL-6 deficiency resulted in a 2.5-fold decrease in tumorigenic potential (Figure 7C), suggesting that autocrine IL-6 contributes to HcPC to HCC progression. To confirm this point, we dispersed freshly isolated DEN-induced aggregates and transduced them with bicistronic lentiviruses encoding either scrambled or IL-6-specific shRNAs and a GFP marker. After a few days in culture, the transduced cells were introduced into MUP-uPA mice that were examined for HCC development 6 months later. Silencing of IL-6 reduced HCC generation (Figure 7D) and inhibited formation of GFP^{+} colonies within the MUP-uPA liver (Figure 7E). We also ablated IL-6 expression in mouse hepatocytes and found that this led to a marked reduction in DEN-induced tumorigenesis (Figure 7F). Thus, autocrine IL-6 production by DEN-initiated HcPC is important for HCC development. To investigate whether autocrine IL-6 signaling also occurs in human premalignant lesions, we examined needle biopsies of normal liver tissue and HCV-infected livers with dysplastic lesions. We found that 16% of all (n = 25) dysplastic lesions exhibited coexpression of LIN28 and IL-6 and contained activated STAT3 (Figure 7G). These markers were hardly detected in normal liver or nontumor portion of HCV-infected livers.

DISCUSSION

The isolation and characterization of cells that can give rise to HCC only after transplantation into an appropriate host liver undergoing chronic injury demonstrates that cancer arises from progenitor cells that are yet to become fully malignant. Importantly, unlike fully malignant HCC cells, the HcPCs we isolated cannot form s.c. tumors or even liver tumors when introduced into a nondamaged liver. Liver damage induced by uPA expression or CCl_4 treatment provides HcPCs with the proper cytokine and growth factor milieu needed for their proliferation. Although HcPCs produce IL-6, they may also depend on other cytokines such as TNF, which is produced by macrophages that are recruited to the damaged liver. In addition, uPA expression and CCl_4 treatment may enhance HcPC growth and progression through their fibrogenic effect on hepatic stellate cells. Although HCC and other cancers have been suspected to arise from

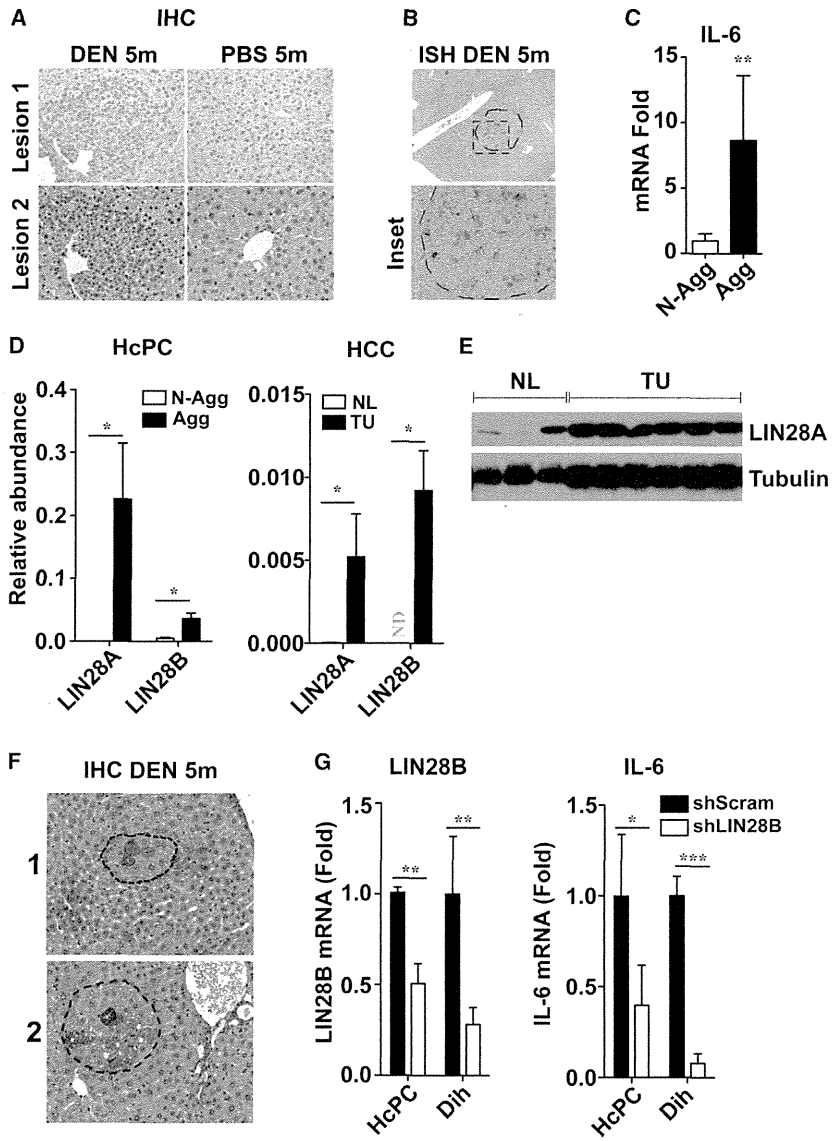

Figure 6. Liver Premalignant Lesions and HcPCs Exhibit Elevated IL-6 and LIN28 Expression

(A and B) Livers of 5-month-old DEN injected mice were analyzed for IL-6 expression by IHC (magnification: 400×) (A) and ISH (magnification: 100×, top; 400×, bottom) (B).

(C and D) Quantification of IL-6 (C) and LIN28 (D) mRNA in aggregated versus nonaggregated hepatocytes from 5-month-old DEN-treated livers and in normal versus tumor-bearing livers (n = 6; ± SEM) (ND, not detected).

(E) Immunoblot analyses of LIN28A in normal (NL) and tumor-bearing (TU) livers.

(F) DEN-treated livers were subjected to IHC with a LIN28A antibody. Broken lines indicate borders of FAH (400×).

(G) LIN28B was silenced with shRNA in HCC (dih) cells and cultured HcPCs, and LIN28B and IL-6 mRNAs were quantitated by qRT-PCR (n = 3; ± SEM).

See also Figure S5 and Table S2.

premalignant/dysplastic lesions (Hruban et al., 2007; Hytiroglou et al., 2007), a direct demonstration that such lesions progress into malignant tumors has been lacking. Based on expression of common markers—EpCAM, CD44, AFP, activated STAT3, and IL-6—that are not expressed in normal hepatocytes, we postulate that HcPCs originate from FAH or dysplastic foci, which are first observed in male mice within 3 months of DEN exposure. Indeed, the cells that are contained within the FAH are smaller than the surrounding parenchyma and are similar in size to isolated HcPCs. Importantly, FAH or premalignant dysplastic foci are not unique to DEN-treated rodents (Bannasch, 1984; Rabes, 1983), and similar lesions were detected in human cirrhotic livers (Hytiroglou et al., 2007; Seki et al., 2000; Takayama et al., 1990) in which the rate of HCC progression is 3%–5% per year (El-Serag, 2011). We found that human dysplastic lesions and mouse FAH and HcPC exhibit autocrine IL-6 signaling. HcPC are not unique to DEN-treated mice, and similar cells were isolated from *Tak1*$^{\Delta hep}$ mice in which HCC development resembles cirrhosis-associated human HCC (Inokuchi et al., 2010).

HcPC Origin and Relationship to Liver and HCC Stem Cells

Transcriptomic analysis indicates that DEN-induced HcPCs are related to both normal hepatobiliary bipotential stem cells/oval cells and HCC cells. Although HcPCs are not fully transformed, they express several markers—CD44, EpCAM, AFP, SOX9, OV6, and CK19—found to be expressed by HCC stem cells and oval cells (Guo et al., 2012; Mikhail and He, 2011; Terris et al., 2010; Yamashita et al., 2008; Zhu et al., 2010). However, unlike oval cells, which do not express albumin or AFP and do not give rise to liver tumors upon transplantation into MUP-uPA mice, HcPCs give rise to HCC after intrasplenic transplantation. Yet, unlike dih10 HCC cells, which express high levels of the HCC stem cell markers AFP, CD44, and EpCAM, HcPCs do not form s.c. tumors.

At this point, it is not clear whether HcPCs arise from oval cells or from dedifferentiated hepatocytes. Given that DEN is metabolically activated by Cyp2E1 that is expressed only in fully differentiated zone 3 hepatocytes (Tsutsumi et al., 1989) and that *Cyp2E1*$^{-/-}$ mice are refractory to DEN (Kang et al., 2007), DEN-induced HcPC are most likely derived from dedifferentiated hepatocytes. Consistent with this hypothesis, DEN-induced FAH and proliferating cells were found in zone 3 and not near bile ducts or the canals of Hering, sites at which oval cells reside

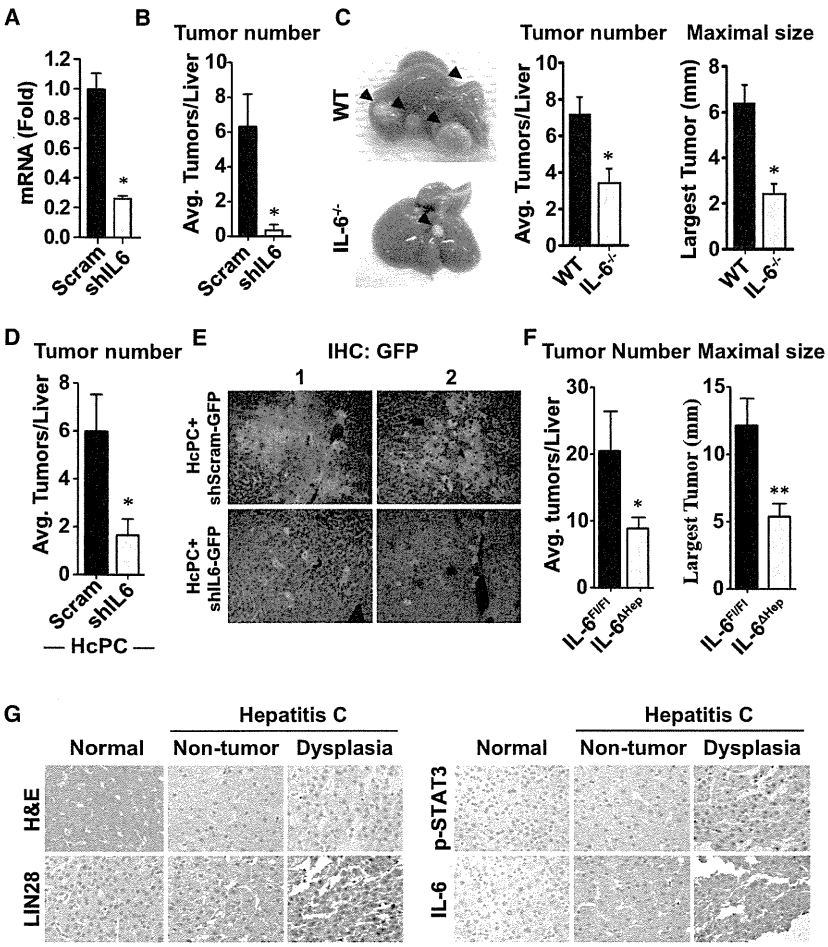

Figure 7. HCC Growth Depends on Autocrine IL-6 Production

(A) HCC cells (dih10) were transduced with lentiviruses containing scrambled or IL-6-specific shRNA. IL-6 mRNA was analyzed by qRT-PCR.

(B) Dih10 cells (1.2×10^5) transduced as above were i.s. injected into MUP-uPA mice that were analyzed 6 months later for HCC development (n = 3; ± SEM).

(C) HcPCs from WT and *Il6*$^{-/-}$ mice were injected (1×10^4 cells/mice) into MUP-uPA mice and analyzed 5 months later for HCC development (n = 5; ± SEM).

(D) HcPCs isolated from DEN-treated WT mice were transduced with shRNA against IL-6 or scrambled shRNA, cultured for 3 to 4 days, i.s. transplanted (1×10^4 cells/mice) into MUP-uPA mice, and analyzed 6 months later (n = 3; ± SEM).

(E) Livers of MUP-uPA mice from (D) were immunostained with GFP antibody 6 months after transplantation (200×). The bicistronic lentivirus in this experiment expresses GFP along with control or IL-6 shRNA, allowing tracking of the infected cells.

(F) DEN-treated *Il6*$^{\Delta hep}$ and *Il6*$^{F/F}$ mice were sacrificed after 9 months to evaluate tumor multiplicity and size (n = 6–10, ± SEM).

(G) IHC analysis of autocrine IL-6 signaling in human premalignant lesions in HCV-infected livers. Expression of LIN28, p-STAT3, and IL-6 was analyzed in 25 needle biopsies of dysplastic nodules, and representative positive specimens (n = 4) are shown. The dysplastic nodules and paired nontumor tissue were obtained from the same HCV-infected patient (n = 25). Nontumor tissue of metastatic liver cancer was used as normal control.

See also Figures S6 and S7.

(Duncan et al., 2009). Notably, GO analysis revealed that many of the genes whose expression is downregulated in HcPC-containing aggregates are involved in xenobiotic and organic acid metabolism, characteristics of differentiated hepatocytes. The same types of genes are also downregulated in HCC. However, final identification of the origin of HcPC will be provided by ongoing lineage-tracing experiments.

The Significance of Autocrine IL-6 Expression

Elevated IL-6 was detected in at least 40% of human HCCs, where it is expressed by the cancer cells (Soresi et al., 2006). More recent studies have confirmed upregulation of IL-6 in human HCC and suggested that it plays a central role in a gene expression network that drives tumor development (Ji et al., 2009). Elevated IL-6 was also found in viral and alcoholic hepatitis and liver cirrhosis, but in these conditions, IL-6 is expressed mainly by myeloid cells/leukocytes rather than parenchymal cells (Deviere et al., 1989; Kakumu et al., 1993; Soresi et al., 2006). Our studies indicate that the critical site of IL-6 expression shifts from myeloid cells to epithelial cells during the course of DEN-induced liver tumorigenesis. Initially, DEN administration rapidly induces IL-6 in Kupffer cells through NF-κB activation (Maeda et al., 2005). This initial surge in IL-6 is required for DEN-induced hepatocarcinogenesis (Naugler et al., 2007). Although IL-6 decays within 2 weeks of DEN administration, it reappears several months later, but at that time, it is expressed within FAH. IL-6 expression is also elevated in isolated HcPCs and is maintained in fully transformed HCC cells. Furthermore, autocrine IL-6 is important for HcPC to HCC progression and for tumorigenic growth. Autocrine IL-6 in both HcPC and HCC cells depends on elevated expression of LIN28, an RNA-binding protein that exerts its protumorigenic activity through downregulation of Let-7, an miRNA that inhibits IL-6 expression (Viswanathan and Daley, 2010). Accordingly, HcPCs exhibit downregulation of both Let-7f and Let-7g, and elevated LIN28 is found not only in isolated HcPCs but also within FAH and human HCV-induced dysplastic lesions.

A similar LIN28-Let-7-IL-6 epigenetic switch is important for in vitro programming and maintenance of cancer stem cells (Iliopoulos et al., 2009). IL-6 also induces malignant features in human ductal carcinoma stem cells (Sansone et al., 2007). In fact, autocrine IL-6 signaling was suggested to play a key role in STAT3-dependent tumor progression (Grivennikov and Karin, 2008). Another miRNA-driven autoregulatory circuit involved in

hepatocarcinogenesis accounts for elevated IL-6R expression (Hatziapostolou et al., 2011). Yet, HcPC-containing aggregates also express several other STAT3-activiting cytokines and receptors. Accordingly, silencing or ablation of IL-6 results in incomplete inhibition of HcPC to HCC progression. Nonetheless, our results demonstrate that autoregulatory circuits/epigenetic switches play an important role in the very early stages of tumorigenesis. Given that such circuits are already activated in premalignant cells, pharmacological agents that disrupt their function may be useful in cancer prevention. Prevention is of particular importance in cancers such as HCC, which is often detected at a stage that is refractory to currently available therapeutics.

EXPERIMENTAL PROCEDURES

Mice, HCC Induction, HcPC Isolation, and Transplantation

MUP-uPA transgenic mice (Weglarz et al., 2000) were maintained on a pure BL/6 background. Because homozygous females frequently die when pregnant, MUP-uPA heterozygotes were generated by backcrossing homozygous MUP-uPA males with BL/6 females to be used as recipients for hepatic transplantation. *Tak1*$^{\Delta hep}$ (Inokuchi et al., 2010) and *Il6*$^{F/F}$ (Quintana et al., 2013) mice were also in the BL/6 background. *Il6*$^{\Delta hep}$ mice were generated by crossing *Il6*$^{F/F}$ and *Alb-Cre* mice. C57BL/6 actin-GFP mice were from the Jackson Laboratories. BL/6 mice were purchased from Charles River Laboratories.

To induce HCC, 15-day-old mice were injected i.p. with 25 mg/kg DEN (Sigma). A pool of DEN-injected BL/6 mice was maintained and used in most experiments. Hepatocytes were isolated using a two-step procedure (He et al., 2010). Cell aggregates were isolated by filtration through 70 and 40 μm sieves. To disperse the aggregates into single cells, they were subjected to gentle pipetting in Ca/Mg-free PBS on ice. Single-cell suspensions of aggregated and nonaggregated hepatocytes were transplanted via an i.s. injection into 21-day-old male MUP-uPA mice (He et al., 2010). Alternatively, single-cell suspensions of aggregated hepatocytes were enriched for CD44^{+} HcPC using magnetic beads. As few as 100 viable CD44^{+} cells mixed with 1 × 10^{5} normal hepatocytes from normal males were transplanted into MUP-uPA mice. Alternatively, BL/6 mice were pretreated with retrorsine (70 mg/kg i.p.) (Sigma), a cell-cycle inhibitor, 1 month prior to transplantation. Transplanted mice were allowed to recover for 1 week and then injected weekly with 3× 0.5 ml/kg CCl_4 i.p. to induce liver injury and hepatocyte proliferation (Guo et al., 2002). Mice were sacrificed 5 to 6 months later, and tumors bigger than 1 mm in diameter on the liver surface were counted. Tumors bigger than 5 mm across were dissected for biochemical and molecular analyses.

ACCESSION NUMBERS

Raw gene expression array data have been deposited to NCBI's Gene Expression Omnibus under the GSE50431 study.

SUPPLEMENTAL INFORMATION

Supplemental Information includes Extended Experimental Procedures, seven figures, and three tables and can be found with this article online at http://dx.doi.org/10.1016/j.cell.2013.09.031.

AUTHOR CONTRIBUTIONS

G.H. identified, isolated, and characterized HcPCs; D.D. and H.N. optimized the HcPC isolation and purification procedure; D.D. found the mechanism of their dependence on autocrine IL-6 controlled by LIN28, characterized them using flow cytometry (with S.S.), and conducted miR analyses (with M.H. and D.I.); H.N. and D.D. used *Il6*$^{\Delta hep}$ mice to demonstrate in vivo HCC dependency on autocrine IL-6; H.N. (with R.T. and K.K.) found IL-6, LIN28, and P-STAT3 in human dysplastic lesions; J.F.-B. conducted the transcriptome analysis and exome sequencing (with S.E.Y., K.J., and O.H.) and with H.O. examined oncogenic potential of oval cells; H.O. examined HcPC proliferative potential and performed IF analysis of isolated HcPC (with A.S. and R.M.H.); Y.J. assisted with IHC and ISH staining; E.S. contributed to the experiments involving *Tak1*$^{\Delta hep}$ mice; G.H., D.D., J.F.-B., H.O., and M.K. wrote the manuscript.

ACKNOWLEDGMENTS

We acknowledge the Biogem facility at UCSD for their assistance with transcriptome analysis and A. Arian, K. Iwaisako, Y. Hiroshima, and H. Matsui for technical assistance. We thank Dr. J. Hidalgo (Universitat Autonoma de Barcelona, Spain) for the *Il6*$^{F/F}$ mice. Research was supported by the Superfund Basic Research Program (P42ES010337), NIH (CA118165 and CA155120), Wellcome Trust (WT086755), American Diabetes Association (7-08-MN-29), the Center for Translational Science (UL1RR031980 and UL1TR000100), the National Center for Research Resources IMAT program (N12R1CA155615), and postdoctoral research fellowships from the Damon Runyon Cancer Research Foundation (G.H.), American Liver Foundation (D.D.), Daiichi Sankyo Foundation of Life Science (H.N.), California Institute for Regenerative Medicine Stem Cell Training Grant II (TG2-01154) fellowship (J.F.-B.), Kanzawa Medical Research Foundation (H.O.), the German Research Foundation (DFG, SH721/1-1 to S.S.), and a Young Investigator Award from the National Childhood Cancer Foundation, "CureSearch" (D.D.). M.K. is an ACS Research Professor and is a recipient of the Ben and Wanda Hildyard Chair for Mitochondrial and Metabolic Diseases.

Received: December 11, 2012
Revised: June 4, 2013
Accepted: September 19, 2013
Published: October 10, 2013

REFERENCES

Bannasch, P. (1984). Sequential cellular changes during chemical carcinogenesis. J. Cancer Res. Clin. Oncol. *108*, 11–22.

Bladt, F., Riethmacher, D., Isenmann, S., Aguzzi, A., and Birchmeier, C. (1995). Essential role for the c-met receptor in the migration of myogenic precursor cells into the limb bud. Nature *376*, 768–771.

Deviere, J., Content, J., Denys, C., Vandenbussche, P., Schandene, L., Wybran, J., and Dupont, E. (1989). High interleukin-6 serum levels and increased production by leucocytes in alcoholic liver cirrhosis. Correlation with IgA serum levels and lymphokines production. Clin. Exp. Immunol. *77*, 221–225.

Dorrell, C., Erker, L., Schug, J., Kopp, J.L., Canaday, P.S., Fox, A.J., Smirnova, O., Duncan, A.W., Finegold, M.J., Sander, M., et al. (2011). Prospective isolation of a bipotential clonogenic liver progenitor cell in adult mice. Genes Dev. *25*, 1193–1203.

Duncan, A.W., Dorrell, C., and Grompe, M. (2009). Stem cells and liver regeneration. Gastroenterology *137*, 466–481.

Eferl, R., Ricci, R., Kenner, L., Zenz, R., David, J.P., Rath, M., and Wagner, E.F. (2003). Liver tumor development. c-Jun antagonizes the proapoptotic activity of p53. Cell *112*, 181–192.

El-Serag, H.B. (2011). Hepatocellular carcinoma. N. Engl. J. Med. *365*, 1118–1127.

Grivennikov, S., and Karin, M. (2008). Autocrine IL-6 signaling: a key event in tumorigenesis? Cancer Cell *13*, 7–9.

Guichard, C., Amaddeo, G., Imbeaud, S., Ladeiro, Y., Pelletier, L., Maad, I.B., Calderaro, J., Bioulac-Sage, P., Letexier, M., Degos, F., et al. (2012). Integrated analysis of somatic mutations and focal copy-number changes identifies key genes and pathways in hepatocellular carcinoma. Nat. Genet. *44*, 694–698.

Guo, D., Fu, T., Nelson, J.A., Superina, R.A., and Soriano, H.E. (2002). Liver repopulation after cell transplantation in mice treated with retrorsine and carbon tetrachloride. Transplantation *73*, 1818–1824.

Guo, X., Xiong, L., Sun, T., Peng, R., Zou, L., Zhu, H., Zhang, J., Li, H., and Zhao, J. (2012). Expression features of SOX9 associate with tumor progression and poor prognosis of hepatocellular carcinoma. Diagn. Pathol. *7*, 44.

Haridass, D., Yuan, Q., Becker, P.D., Cantz, T., Iken, M., Rothe, M., Narain, N., Bock, M., Nörder, M., Legrand, N., et al. (2009). Repopulation efficiencies of adult hepatocytes, fetal liver progenitor cells, and embryonic stem cell-derived hepatic cells in albumin-promoter-enhancer urokinase-type plasminogen activator mice. Am. J. Pathol. *175*, 1483–1492.

Hatziapostolou, M., Polytarchou, C., Aggelidou, E., Drakaki, A., Poultsides, G.A., Jaeger, S.A., Ogata, H., Karin, M., Struhl, K., Hadzopoulou-Cladaras, M., and Iliopoulos, D. (2011). An HNF4α-miRNA inflammatory feedback circuit regulates hepatocellular oncogenesis. Cell *147*, 1233–1247.

He, G., Yu, G.Y., Temkin, V., Ogata, H., Kuntzen, C., Sakurai, T., Sieghart, W., Peck-Radosavljevic, M., Leffert, H.L., and Karin, M. (2010). Hepatocyte IKKbeta/NF-kappaB inhibits tumor promotion and progression by preventing oxidative stress-driven STAT3 activation. Cancer Cell *17*, 286–297.

Hruban, R.H., Maitra, A., Kern, S.E., and Goggins, M. (2007). Precursors to pancreatic cancer. Gastroenterol. Clin. North Am. *36*, 831–849, vi.

Hytiroglou, P., Park, Y.N., Krinsky, G., and Theise, N.D. (2007). Hepatic precancerous lesions and small hepatocellular carcinoma. Gastroenterol. Clin. North Am. *36*, 867–887, vii.

Ichinohe, N., Kon, J., Sasaki, K., Nakamura, Y., Ooe, H., Tanimizu, N., and Mitaka, T. (2012). Growth ability and repopulation efficiency of transplanted hepatic stem cells, progenitor cells, and mature hepatocytes in retrorsine-treated rat livers. Cell Transplant. *21*, 11–22.

Iliopoulos, D., Hirsch, H.A., and Struhl, K. (2009). An epigenetic switch involving NF-kappaB, Lin28, Let-7 MicroRNA, and IL6 links inflammation to cell transformation. Cell *139*, 693–706.

Inokuchi, S., Aoyama, T., Miura, K., Osterreicher, C.H., Kodama, Y., Miyai, K., Akira, S., Brenner, D.A., and Seki, E. (2010). Disruption of TAK1 in hepatocytes causes hepatic injury, inflammation, fibrosis, and carcinogenesis. Proc. Natl. Acad. Sci. USA *107*, 844–849.

Ji, J., Shi, J., Budhu, A., Yu, Z., Forgues, M., Roessler, S., Ambs, S., Chen, Y., Meltzer, P.S., Croce, C.M., et al. (2009). MicroRNA expression, survival, and response to interferon in liver cancer. N. Engl. J. Med. *361*, 1437–1447.

Kakumu, S., Shinagawa, T., Ishikawa, T., Yoshioka, K., Wakita, T., and Ida, N. (1993). Interleukin 6 production by peripheral blood mononuclear cells in patients with chronic hepatitis B virus infection and primary biliary cirrhosis. Gastroenterol. Jpn. *28*, 18–24.

Kang, J.S., Wanibuchi, H., Morimura, K., Gonzalez, F.J., and Fukushima, S. (2007). Role of CYP2E1 in diethylnitrosamine-induced hepatocarcinogenesis in vivo. Cancer Res. *67*, 11141–11146.

Laconi, E., Oren, R., Mukhopadhyay, D.K., Hurston, E., Laconi, S., Pani, P., Dabeva, M.D., and Shafritz, D.A. (1998). Long-term, near-total liver replacement by transplantation of isolated hepatocytes in rats treated with retrorsine. Am. J. Pathol. *153*, 319–329.

Maeda, S., Kamata, H., Luo, J.L., Leffert, H., and Karin, M. (2005). IKKbeta couples hepatocyte death to cytokine-driven compensatory proliferation that promotes chemical hepatocarcinogenesis. Cell *121*, 977–990.

Marquardt, J.U., and Thorgeirsson, S.S. (2010). Stem cells in hepatocarcinogenesis: evidence from genomic data. Semin. Liver Dis. *30*, 26–34.

Meyer, K., Lee, J.S., Dyck, P.A., Cao, W.Q., Rao, M.S., Thorgeirsson, S.S., and Reddy, J.K. (2003). Molecular profiling of hepatocellular carcinomas developing spontaneously in acyl-CoA oxidase deficient mice: comparison with liver tumors induced in wild-type mice by a peroxisome proliferator and a genotoxic carcinogen. Carcinogenesis *24*, 975–984.

Mikhail, S., and He, A.R. (2011). Liver cancer stem cells. Int. J. Hepatol. *2011*, 486954.

Naugler, W.E., Sakurai, T., Kim, S., Maeda, S., Kim, K., Elsharkawy, A.M., and Karin, M. (2007). Gender disparity in liver cancer due to sex differences in MyD88-dependent IL-6 production. Science *317*, 121–124.

Nguyen, L.V., Vanner, R., Dirks, P., and Eaves, C.J. (2012). Cancer stem cells: an evolving concept. Nat. Rev. Cancer *12*, 133–143.

Nowell, P.C. (1976). The clonal evolution of tumor cell populations. Science *194*, 23–28.

Park, E.J., Lee, J.H., Yu, G.Y., He, G., Ali, S.R., Holzer, R.G., Osterreicher, C.H., Takahashi, H., and Karin, M. (2010). Dietary and genetic obesity promote liver inflammation and tumorigenesis by enhancing IL-6 and TNF expression. Cell *140*, 197–208.

Pitot, H.C. (1990). Altered hepatic foci: their role in murine hepatocarcinogenesis. Annu. Rev. Pharmacol. Toxicol. *30*, 465–500.

Porta, C., De Amici, M., Quaglini, S., Paglino, C., Tagliani, F., Boncimino, A., Moratti, R., and Corazza, G.R. (2008). Circulating interleukin-6 as a tumor marker for hepatocellular carcinoma. Ann. Oncol. *19*, 353–358.

Quintana, A., Erta, M., Ferrer, B., Comes, G., Giralt, M., and Hidalgo, J. (2013). Astrocyte-specific deficiency of interleukin-6 and its receptor reveal specific roles in survival, body weight and behavior. Brain Behav. Immun. *27*, 162–173.

Rabes, H.M. (1983). Development and growth of early preneoplastic lesions induced in the liver by chemical carcinogens. J. Cancer Res. Clin. Oncol. *106*, 85–92.

Rhim, J.A., Sandgren, E.P., Degen, J.L., Palmiter, R.D., and Brinster, R.L. (1994). Replacement of diseased mouse liver by hepatic cell transplantation. Science *263*, 1149–1152.

Sansone, P., Storci, G., Tavolari, S., Guarnieri, T., Giovannini, C., Taffurelli, M., Ceccarelli, C., Santini, D., Paterini, P., Marcu, K.B., et al. (2007). IL-6 triggers malignant features in mammospheres from human ductal breast carcinoma and normal mammary gland. J. Clin. Invest. *117*, 3988–4002.

Seki, S., Sakaguchi, H., Kitada, T., Tamori, A., Takeda, T., Kawada, N., Habu, D., Nakatani, K., Nishiguchi, S., and Shiomi, S. (2000). Outcomes of dysplastic nodules in human cirrhotic liver: a clinicopathological study. Clin. Cancer Res. *6*, 3469–3473.

Sell, S., and Leffert, H.L. (2008). Liver cancer stem cells. J. Clin. Oncol. *26*, 2800–2805.

Shin, S., Walton, G., Aoki, R., Brondell, K., Schug, J., Fox, A., Smirnova, O., Dorrell, C., Erker, L., Chu, A.S., et al. (2011). Foxl1-Cre-marked adult hepatic progenitors have clonogenic and bilineage differentiation potential. Genes Dev. *25*, 1185–1192.

Soresi, M., Giannitrapani, L., D'Antona, F., Florena, A.M., La Spada, E., Terranova, A., Cervello, M., D'Alessandro, N., and Montalto, G. (2006). Interleukin-6 and its soluble receptor in patients with liver cirrhosis and hepatocellular carcinoma. World J. Gastroenterol. *12*, 2563–2568.

Su, Y., Kanamoto, R., Miller, D.A., Ogawa, H., and Pitot, H.C. (1990). Regulation of the expression of the serine dehydratase gene in the kidney and liver of the rat. Biochem. Biophys. Res. Commun. *170*, 892–899.

Su, Q., Benner, A., Hofmann, W.J., Otto, G., Pichlmayr, R., and Bannasch, P. (1997). Human hepatic preneoplasia: phenotypes and proliferation kinetics of foci and nodules of altered hepatocytes and their relationship to liver cell dysplasia. Virchows Arch. *431*, 391–406.

Takayama, T., Makuuchi, M., Hirohashi, S., Sakamoto, M., Okazaki, N., Takayasu, K., Kosuge, T., Motoo, Y., Yamazaki, S., and Hasegawa, H. (1990). Malignant transformation of adenomatous hyperplasia to hepatocellular carcinoma. Lancet *336*, 1150–1153.

Terris, B., Cavard, C., and Perret, C. (2010). EpCAM, a new marker for cancer stem cells in hepatocellular carcinoma. J. Hepatol. *52*, 280–281.

Tsutsumi, M., Lasker, J.M., Shimizu, M., Rosman, A.S., and Lieber, C.S. (1989). The intralobular distribution of ethanol-inducible P450IIE1 in rat and human liver. Hepatology *10*, 437–446.

Verna, L., Whysner, J., and Williams, G.M. (1996). N-nitrosodiethylamine mechanistic data and risk assessment: bioactivation, DNA-adduct formation, mutagenicity, and tumor initiation. Pharmacol. Ther. *71*, 57–81.

Viswanathan, S.R., and Daley, G.Q. (2010). Lin28: A microRNA regulator with a macro role. Cell *140*, 445–449.

Wang, R., Ferrell, L.D., Faouzi, S., Maher, J.J., and Bishop, J.M. (2001). Activation of the Met receptor by cell attachment induces and sustains hepatocellular carcinomas in transgenic mice. J. Cell Biol. *153*, 1023–1034.